Angewandte Chemie
Eine Zeitschrift der Gesellschaft Deutscher Chemiker

Supporting Information

69451 Weinheim, Germany

Unprecedented Immunosuppressive Polyketides from *Daldinia eschscholzii*, a Mantis-associated Fungus

Ying Lao Zhang, Hui Ming Ge, Wei Zhao, Hao Dong, Qiang Xu, Shu Hua Li, Jing Li, Jie Zhang, Yong Chun Song, Ren Xiang Tan*

List of Supporting Information

1. Strain and cultivation

According to the methods detailed elsewhere,[1] the strain IFB-TL01 was isolated from the gut of *T. aridifolia* collected in Oct. 2005 from the Zijin Mountain in the suburb of Nanjing, China. The strain was identified by comparing the morphological character and 18S rDNA sequence with that of standard record. The experimental data and observations led to the identification of the strain as *D. eschscholzii*, which was deposited in the China Center for Type Culture Collection (CCTCC) under the number M207198. The fresh mycelium of *D. Eschscholzii* was inoculated into 500 mL flask containing 100 mL of ME medium (consisting of 20 g malt extract, 20 g sucrose, 1 g peptone in 1 L of distilled water). After 2 d of incubation at 28 °C with an agitation of 150 rpm, 50 mL of culture liquid was transferred as seed into each 1 L flask containing 500 mL of ME medium. Cultivation was kept at 28 °C with an agitation of 150 rpm for 10 d. The procedure was repeated until sufficient biomass was accumulated.

2. Isolation of metabolites 1, 2, 5, 8

The filtrate of the culture broth (100 L) was extracted exhaustively with ethyl acetate. Evaporation of solvent *in vacuo* gave a brown oily residue (35.0 g) which gave seven fractions upon silica gel column chromatography ($CHCl_3$/MeOH, gradient 100:0→25:8). The first active fraction was subjected to silica gel chromatography using $CHCl_3$, followed by gel filtration over Sephadex LH20 with $CHCl_3$:MeOH (1:1) and recrystallization in MeOH to yield dalesconol A (**1**) (100.2 mg). The second active fraction was purified again by silica gel chromatography ($CHCl_3$/MeOH gradient, 100:0.5 to 100:1) and subsequent gel filtration over Sephadex LH20 with $CHCl_3$:MeOH (1:1) and then recrystallization in MeOH to yield dalesconol B (**2**) (70.9 mg) and **5** (98.9 mg). The third fraction was also purified by column chromatography fractionation over silica gel with $CHCl_3$:MeOH (100:2) and then further purified by Sephadex LH-20 with MeOH to provide **8** (5.0 mg).

3. Optical resolution of dalesconols A (1) and B (2) by chiral HPLC

The chiral HPLC preparation of pure enantiomers were accomplished for **1** over a Chiralpak AS-H (column size: 4.6 × 250 mm; Daicel Chemical Ltd; column temperature: 35 °C; mobile phase: Hexane/2-propanol/HAc=60/40/0.1 (v/v/v); flow rate: 0.6 mL/min), and for **2** over Chiralpak IA (column size: 4.6×250 mm; Daicel Chemical Ltd; column temperature: 35 °C; mobile phase: MtBE/THF/HAc =95/5/0.1 (v/v/v); flow rate: 1.0 mL/min) columns. The retention time of the four single enantiomers was 31.43 [(+)-**1**], 46.08 [(-)-**1**], 22.75 [(+)-**2**] and 30.09 min [(-)-**2**], respectively. After the optical resolution, the optical purity (>99% ee) was checked in the same HPLC conditions.

The chiral HPLC analysis of **1** and **2** obtained from direct HPLC collection were performed for the former over a Chiralpak ASH (column size: 4.6×250 mm; Daicel Chemical Ltd; column temperature: 40 °C; mobile phase: *n*-Hexane/2-propanol/HAc, 60/40/0.1, v/v/v; flow rate: 0.6 mL/min), and for the later over Chiralpak ASH (column size: 4.6×250 mm; Daicel Chemical Ltd; column temperature: 40 °C; mobile phase: *n*-Hexane/2-propanol/HAc, 80/20/0.1, v/v/v; flow rate: 1.0 mL/min) columns. In these conditions, the retention time of the four single enantiomers was 30.4 [(+)-**1**], 36.6 [(-)-**1**], 22.6 [(+)-**2**] and 26.2 min [(-)-**2**], respectively.

4. Biosynthetic studies

Stable isotope label feeding experiments with *D. eschscholzii* were performed according to the protocol used for the production and isolation of dalesconols A (**1**) and B (**2**) with small modification. Thus, at 24, 32 and 40 h after inoculation, sodium [1-^{13}C]acetate (200 mg/200 mL of media × 5 flasks) was added in thirds in a sterile

manner through millipore filters (0.2 μm). Fractionation after 20 d culture yielded the labeled products **1a** (4.5 mg) and **2a** (3.5 mg). A similar experiment employing sodium [2-^{13}C]acetate and [1,2-^{13}C2]acetate gave the two differentially labeled pair of **1b** (4.6 mg), **2b** (3.3 mg), **1c** (4.5 mg) and **2c** (3.5 mg), respectively.

5. Computational details

For these systems, we first carried out full geometry optimizations at the B3LYP level with the standard TZVP basis set. Then, the corresponding excited-state calculations were performed at the ground-state optimized geometries. Time-dependent DFT (TD-DFT) with the same basis set was employed to calculate the spin-allowed excitation energies, rotatory (R_n) and oscillator strengths (f_n) of the lowest 120 excited states. The final ECD spectra was obtained as a sum of Gaussians centered at the wavelengths of the corresponding electronic transitions and multiplied with their rotatory strengths. The peak intensity Δε(λ) (in L mol^{-1} cm^{-1}) was calculated according to the following equation.[2]

$$\Delta\varepsilon(\lambda) = \sum_n \frac{\lambda_n R_n}{22.94\Delta\lambda_n\sqrt{\pi}} \times 10^{40} \exp\left[-\left(\frac{\lambda-\lambda_n}{\Delta\lambda_n}\right)^2\right]$$

where λ_n was the wavelength of the nth transition, and $\Delta\lambda_n$ was the half-width at the 1/*e* of peak maximum. Here, we used a half-width $\Delta\lambda_n = \lambda_n^2\Delta\tilde{\upsilon}$ with $\Delta\tilde{\upsilon} = 850cm^{-1}$. All the calculations have been done using the TURBOMOLE V5.8 program package.[3]

6. Biological testing

The *in vitro* immunosuppressive activity and cytotoxicity were evaluated by the T cell viability and MTT assays as described in our previous papers.[4-5]

7. Spectral data of dalesconol A (1)

Red crystals, m.p. 308-309 °C; UV (MeOH): λ_{max} nm (logε)=462 (3.89), 338 (4.17), 206 (4.51); IR (KBr) ν_{max}: 3063.1, 3036.1, 2958.5, 2910.4, 1644.7, 1629.6, 1608.6, 1585.9, 1552.0, 1518.8, 1473.8, 1452.6, 1411.8, 1396.0, 1266.7, 1216.6, 1161.3, 852.0, 820.9, 772.8 cm^{-1}; HRESIMS: *m/z* 463.1180 [*M*+H]$^+$, calcd for $C_{29}H_{19}O_6$, 463.1176; ^{1}H and ^{13}C NMR data: see Tables S1 and S3. (–)-**1**: $[\alpha]^{20}_D$= –487.8°(*c*=0.07 in MeCN); CD (MeCN): λ_{max} nm ($\Delta\varepsilon$)=216 (+52.52), 233.2 (–27.16), 265.1 (+11.33), 320.1 (–4.62). (+)-**1**: $[\alpha]^{20}_D$= +485.9° (*c*=0.07 in MeCN); CD (MeCN): λ_{max} nm ($\Delta\varepsilon$)=216 (–55.18), 233.1 (+28.79), 265.4 (–11.60), 323.1 (+4.75).

8. Spectral data of dalesconol B (2)

Red needles, m.p. 344-346 °C; UV (MeOH): λ_{max} nm (logε)=459 (3.80), 337 (4.08), 206 (4.46); IR (KBr) ν_{max}: 3177.1, 3068.1, 2923.4, 2852.6, 1648.6, 1611.8, 1558.0, 1523.6, 1475.1, 1450.3, 1219.5, 1198.6, 1167.4, 846.2 cm^{-1}; MS (EI): *m/z* (%): 478.1 (100) [*M*]$^+$, 418.1 (20), 417.1 (35), 410.1 (30); HRMS (EI): *m/z* calcd for $C_{29}H_{18}O_7$ [*M*]$^+$: 478.1053; found: 478.1062. ^{1}H and ^{13}C NMR data: see Tables S1 and S3. (–)-**2**: $[\alpha]^{20}_D$ = –613.8° (*c*=0.04 in MeCN); CD (MeCN): λ_{max} nm ($\Delta\varepsilon$)=215.2 (+41.41), 247.5 (–10.84), 296.7 (+19.21), 346.1 (–6.09). (+)-**2**: $[\alpha]^{20}_D$ = +613.4° (*c*=0.03 in MeCN); CD (MeCN): λ_{max} nm ($\Delta\varepsilon$)=215.1 (–43.69), 248.1 (+11.62), 296.9 (–20.75), 345.3 (+6.75).

9. Dibromobenzenesulfonation of dalesconol A (1)

To a solution of 4.0 mg (8.66×10^{-3} mmol) of **1** in 5 mL of pyridine was added 8.8 mg (3.46×10^{-2} mmol) of *p*-bromobenzenesulfonyl chloride. The mixture was stirred for 24 h at room temperature and then concentrated *in vacuo*. The residue was purified by Sephadex LH-20 to provide **1'** (6.9 mg) as a yellow powder: m.p. 171-

173 °C; UV (MeCN): λ_{max} nm (logε)=370 (1.79), 312 (1.71), 235 (2.25); ^{1}H NMR ($CDCl_3$, 500 MHz): δ=12.62 (s, -OH), 8.01 (d, *J*=8.3 Hz, 2H), 7.73 (d, *J*=8.3 Hz, 2H), 7.69 (m, 4H), 7.61 (t, *J*=7.9 Hz, 1H), 7.44 (d, *J*=7.5 Hz, 1H), 7.37 (d, *J*=9.9 Hz, 1H), 7.32 (m, 3H), 7.23 (d, *J*=7.9 Hz, 1H), 6.91 (d, *J*=8.3 Hz, 1H), 6.64 (d, *J*=9.9 Hz, 1H), 6.21 (d, *J*=7.4 Hz, 1H), 3.61 (dd, *J*=18.5, 4.8 Hz, 1H), 3.16 (t, *J*=11.9 Hz, 1H), 2.85 (m, 3H); ESI(+)MS *m/z* 901/903/905 ([*M*+H]$^+$), 923/925/927 ([*M*+Na]$^+$).

Table S1. ^{1}H NMR (500 MHz, 25 °C) data of **1** and **2** in DMSO-d_6.

position	**1** δ_H mult. (*J*, Hz)	**2** δ_H mult. (*J*, Hz)
4	6.92 d (8.0)	6.18 d (1.9)
5	7.54 dd (8.0,8.0)	
6	7.17 d (8.0)	6.55 d (1.9)
10	8.04 d (9.8)	8.01 d (9.8)
11	6.81 d (9.8)	6.81 d (9.8)
15	6.80 d (8.2)	6.81 d (8.3)
16	7.70 d (8.2)	7.68 d (8.3)
21	5.89 d (8.0)	5.88 d (8.0)
22	7.09 dd (8.0,8.0)	7.14 t (8.0)
23	6.67 d (8.0)	6.67 d (8.0)
27	α: 2.87 dd (17.0, 2.2)	2.81 dd (16.8, 3.5)
	β: 3.62 dd (17.0, 6.4)	3.51 dd (16.8, 6.5)
28	2.82 m	2.90 m
29	α: 3.39 dd (12.7, 7.8)	3.29 dd (13.2, 7.5)
	β: 2.77 dd (12.7, 2.9)	2.62 dd (13.2, 1.9)
3 –OH	11.50 s	12.39 s
14 -OH	10.69 s	10.66 s
24 -OH	12.28 s	12.18 s
5 –OH		10.95 br s

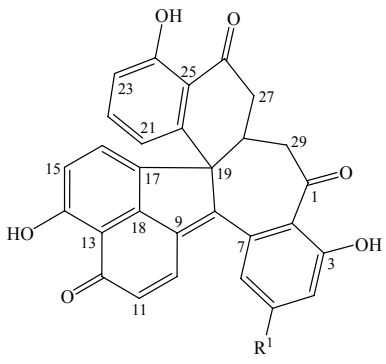

1: R^1 = H **2**: R^1 = OH

Table S2. TDDFT based results for the optimized conformer of (–)-**1** (350nm>λ>200nm).

Transition	Excitation Energy[a] (nm)	Rotatory Strength R^b (10^{-40} cgs)	Oscillator Strength f^b	Dominant Contributions[c]	Weight
11	327	-74.568	0.122	112-121 113-121	0.622 0.172
17	287	37.645	0.019	111-121 117-122	0.591 0.109
21	275	-26.624	0.065	120-125 120-124	0.661 0.150
22	270	79.841	0.057	117-123 117-122 111-121	0.381 0.248 0.133
27	256	-16.329	0.017	119-124	0.854
28	253	22.126	0.022	115-123 116-123 115-122	0.426 0.161 0.154
31	247	45.024	0.023	114-123 112-122 113-122	0.213 0.210 0.133
32	246	46.659	0.021	112-123 113-123 114-123	0.390 0.140 0.135
33	245	-67.003	0.046	120-127 114-123 112-122	0.460 0.141 0.125
34	244	-38.986	0.074	119-125 112-123 113-123 120-127	0.265 0.199 0.122 0.102
38	231	24.358	0.046	111-122 120-128 117-124	0.323 0.115 0.107
41	229	23.039	0.004	109-121 120-128 111-123	0.473 0.175 0.109
42	228	31.802	0.042	109-121 111-123 119-127	0.317 0.224 0.179
47	221	-53.606	0.056	117-125 119-127 119-126	0.375 0.156 0.154
48	220	74.094	0.047	117-125 118-126 119-126	0.246 0.210 0.139
51	215	52.141	0.050	118-126 118-127	0.490 0.101
54	212	24.129	0.058	114-124 119-128 118-127	0.321 0.199 0.160
55	211	-32.822	0.042	118-127 104-121 106-121	0.228 0.144 0.101
59	208	-16.444	0.036	120-129 119-128	0.546 0.152
61	206	18.654	0.027	104-121 112-124 117-126	0.185 0.115 0.111
63	205	76.938	0.021	104-121 117-127 114-125	0.256 0.199 0.147
65	204	58.154	0.067	117-127 112-124 113-124 103-121	0.243 0.211 0.139 0.114
67	201	33.275	0.010	120-130 118-128 119-129	0.247 0.209 0.102

[a] Excited states with $f < 0.1$ and $R < \pm 16.0$ were not presented.
[b] All the strengths were in the velocity representation.
[c] Configurations with weights below 0.10 were not displayed.

Table S3. ^{13}C enrichment in dalesconols A (**1**) and B (**2**) after feeding [1-^{13}C] and [2-^{13}C]acetates.

C no.	**1** δ_C[a]	**1a**[b]	**1b**[c]	**2** δ_C[a]	**2a**[b]	**2b**[c]
1	206.3	**7.3**	0.9	204.4	**3.7**	0.6
2	120.7	1.2	**3.9**	113.0	0.8	**3.4**
3	161.3	**4.8**	0.8	165.7	**3.4**	0.6
4	120.4	1.0	**3.1**	104.7	0.7	**7.0**
5	136.3	**8.5**	1.0	164.6	**2.8**	0.6
6	126.6	0.5	**3.2**	115.5	1.6	**5.6**
7	136.9	**11.1**	1.0	139.4	**5.5**	1.0
8	163.5	1.2	**2.9**	163.6	1.1	**3.1**
9	142.6	0.8	**2.2**	132.8	1.0	**2.9**
10	136.1	**8.3**	1.0	135.7	**6.5**	1.6
11	133.7	1.4	**2.3**	133.7	1.6	**5.2**
12	189.2	**7.3**	1.3	189.2	**3.4**	1.0
13	114.4	0.8	**2.6**	114.4	0.7	**2.6**
14	159.2	**3.6**	0.9	159.1	**2.7**	0.6
15	115.5	1.4	**2.7**	115.7	1.2	**5.6**
16	129.4	**8.4**	1.0	129.2	**7.0**	1.7
17	133.1	1.4	**2.7**	143.1	1.0	**3.1**
18	144.6	**8.9**	1.2	144.8	**3.8**	1.4
19	64.9	0.8	**3.4**	64.7	0.5	**3.1**
20	142.2	**5.7**	1.0	142.3	**4.1**	0.7
21	119.9	1.0	**3.0**	119.7	1.0	**5.6**
22	138.4	**3.8**	0.8	138.3	**3.7**	1.3
23	117.4	1.1	**3.1**	117.2	1.4	**5.0**
24	162.2	**3.8**	0.9	162.0	**3.0**	0.5
25	118.3	0.6	**3.1**	118.3	1.0	**3.4**
26	203.6	**5.4**	0.9	203.6	**3.3**	0.6
27	43.7	1.2	**3.4**	42.3	1.2	**5.0**
28	38.6	**11.2**	1.4	37.3	**5.9**	1.2
29	51.7	0.9	**3.4**	51.0	1.2	**6.3**

[a] The proton-decoupled ^{13}C NMR spectra (125 MHz) were measured in DMSO-d_6. [b] In feeding of [1-^{13}C]acetate, all signals were referenced to the peak height of the ^{13}C-21 signal. The numbers in boldface refer to the unequivocal incorporation of the corresponding precursor. [c] In feeding of [2-^{13}C]acetate, all signals were referenced to the peak height of the ^{13}C-7 signal.

Table S4. ^1Jcc values (Hz) revealed by a feeding experiment with [1,2-$^{13}C_2$]acetate

^1Jcc	**1**	**2**	^1Jcc	**1**	**2**
J_{C1C29}	39	35	J_{C14C15}	65	64
J_{C2C3}	64	64	J_{C16C17}	59	59
J_{C4C5}	54	67	J_{C19C28}	31	31
J_{C6C7}	57	59	J_{C20C21}	56	57
J_{C9C18}	52	52	J_{C22C23}	60	61
J_{C10C11}	57	58	J_{C24C25}	64	64
J_{C12C13}	55	55	J_{C26C27}	34	34

Table S5. *In vitro* inhibitory effects of dalesconols and their precursors on ConA-induced proliferation of mouse spleen cells.

compounds	IC_{50} (μg mL^{-1})		SI[b]
	ConA-induced	Cytotoxicity	
dalesconol A (**1**)	0.16	>80	>500
(+)-dalesconol A [(+)-**1**]	0.29	>80	>276
(–)-dalesconol A [(–)-**1**]	0.58	>80	>138
dalesconol B (**2**)	0.25	>80	>320
(+)-dalesconol B [(+)-**2**]	0.47	>80	>170
(–)-dalesconol B [(–)-**2**]	0.47	>80	>170
5	18.35	N/T[c]	
8	18.33	N/T	
cyclosporin A[a]	0.06	11.2	187

[a] Co-assayed as a positve control. [b] Selectivity index [SI] determined as the ratio of the IC_{50} values on resting mouse spleen cells viability (cytotoxicity) to the IC_{50} on the activated proliferation of mouse spleen cells. [c] Not tested.

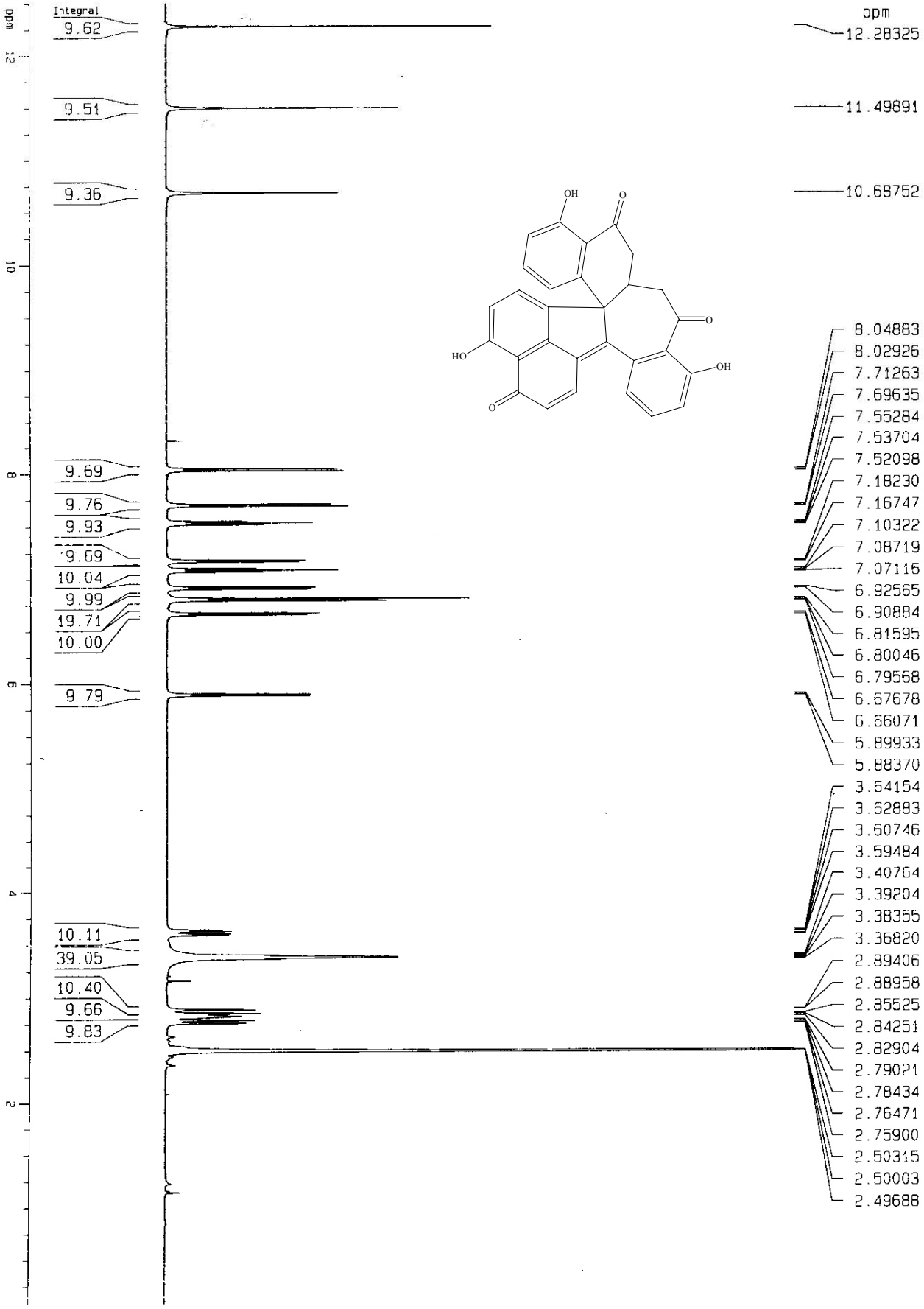

Figure S1. The ^{1}H NMR spectrum of **1** in DMSO-d_6 (500MHz).

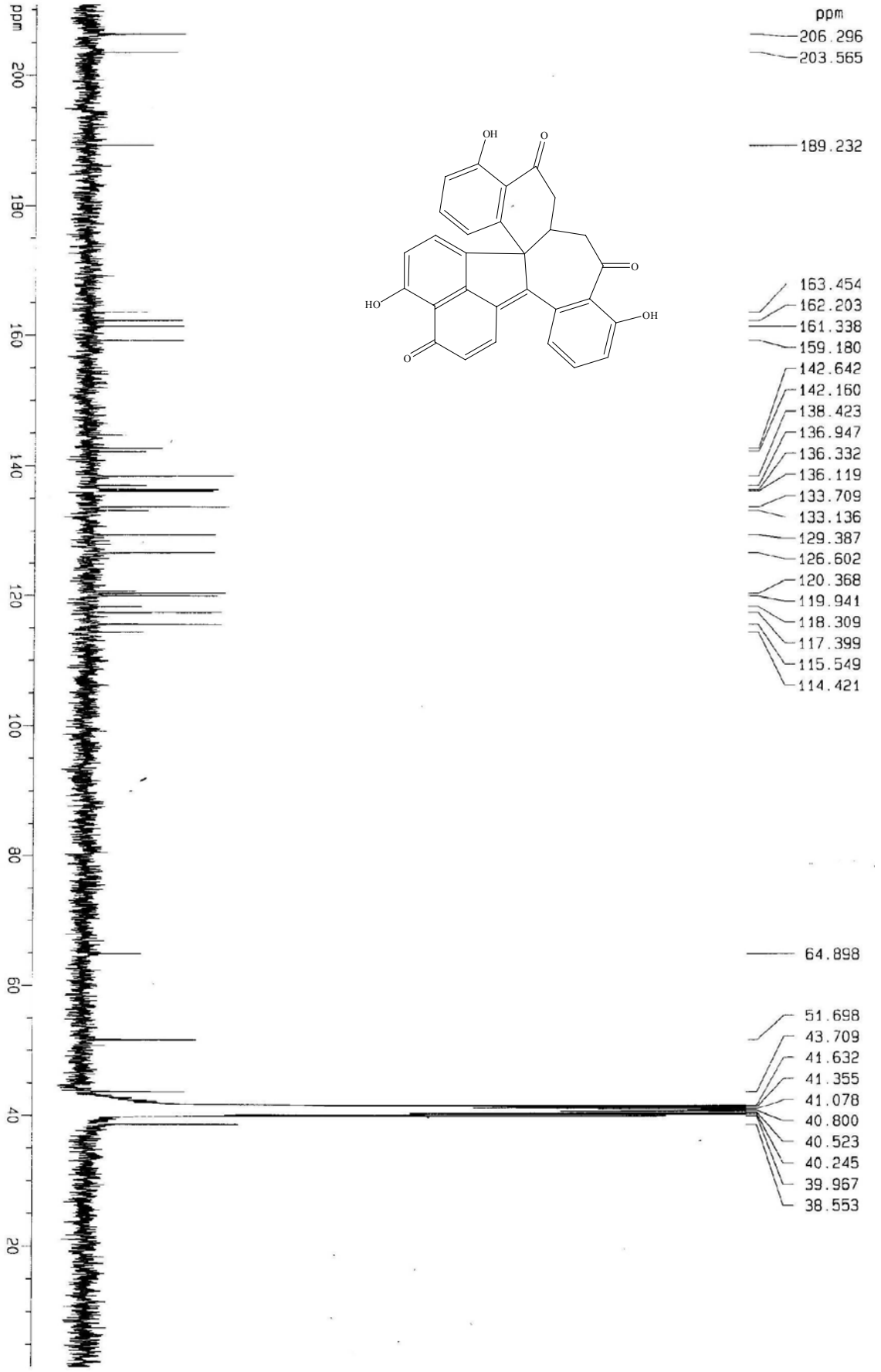

Figure S2. The ^{13}C NMR spectrum of **1** in DMSO-d_6 (75MHz).

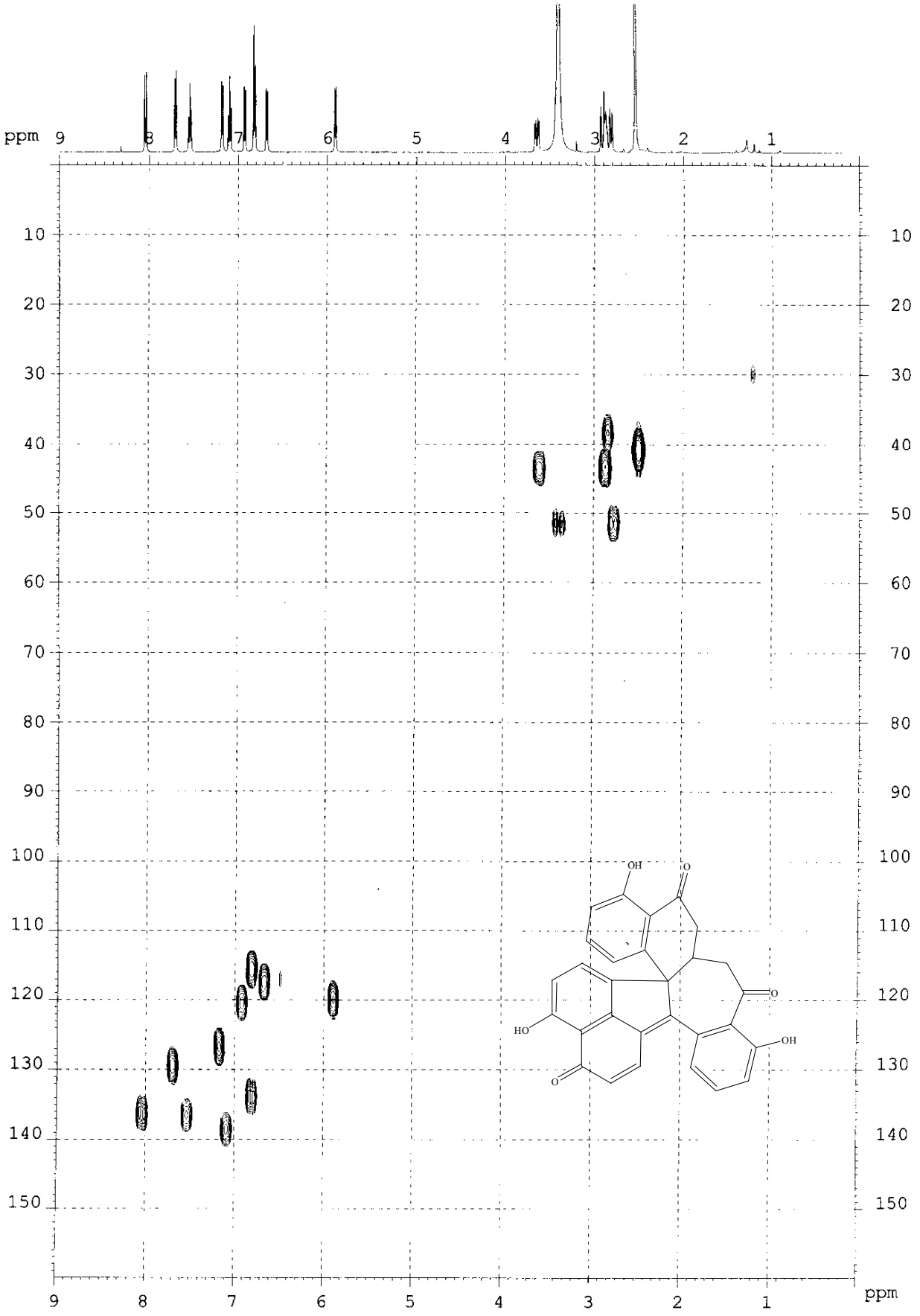

Figure S3. The HMQC spectrum of **1** in DMSO-d_6 (500MHz).

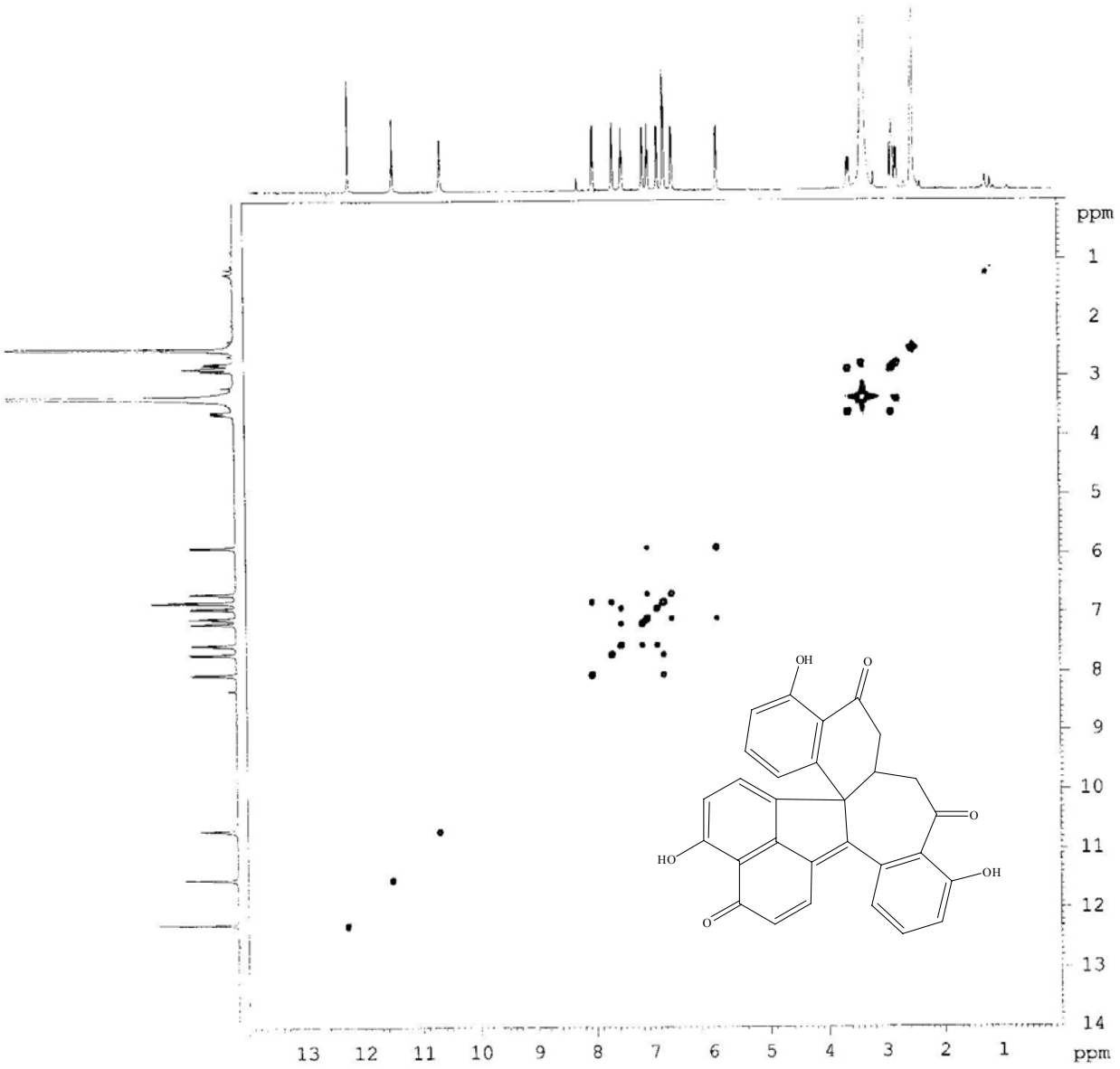

Figure S4. The ^{1}H-^{1}H COSY spectrum of **1** in DMSO-d_6 (500MHz).

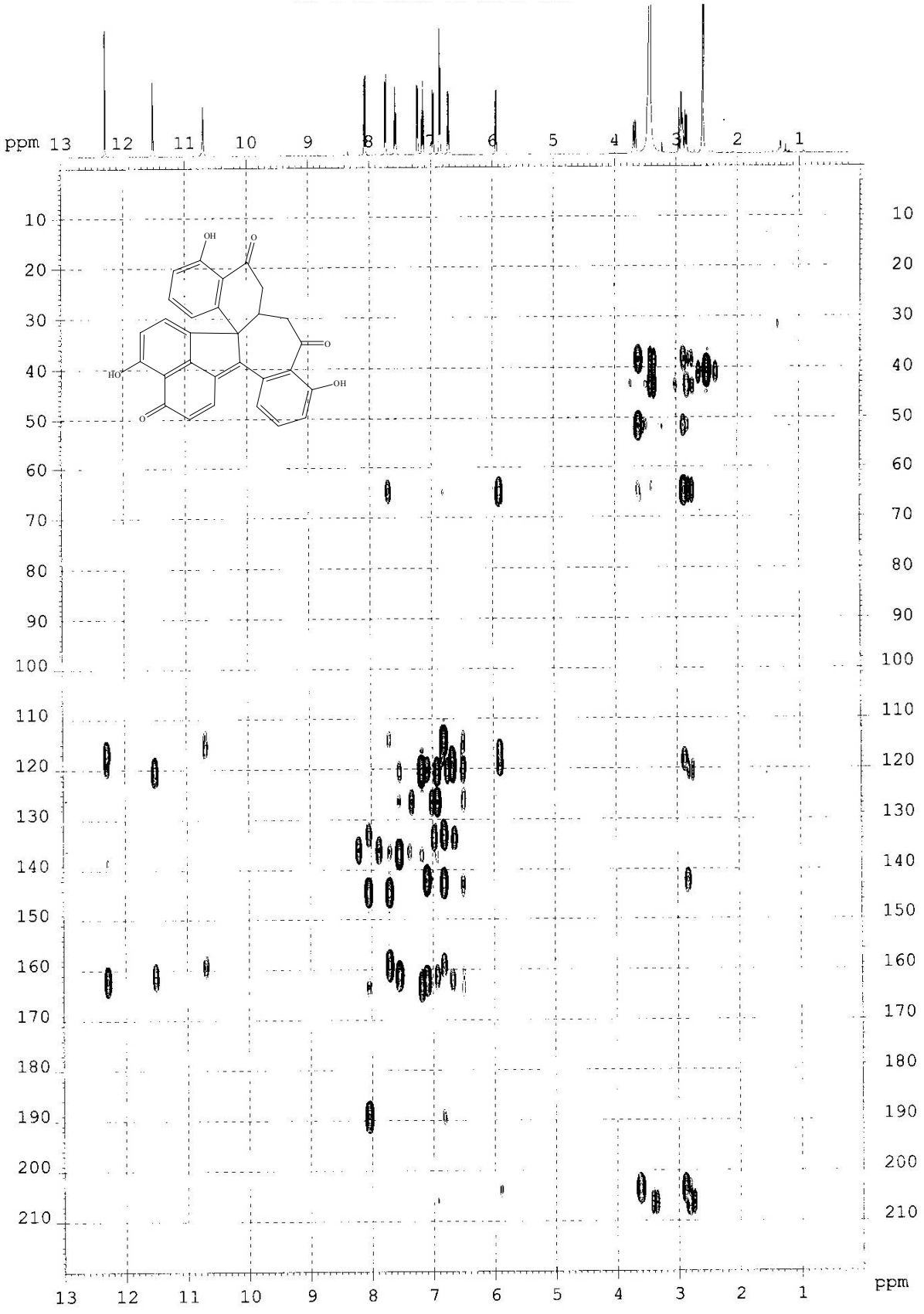

Figure S5. The HMBC spectrum of **1** in DMSO-d_6 (500MHz).

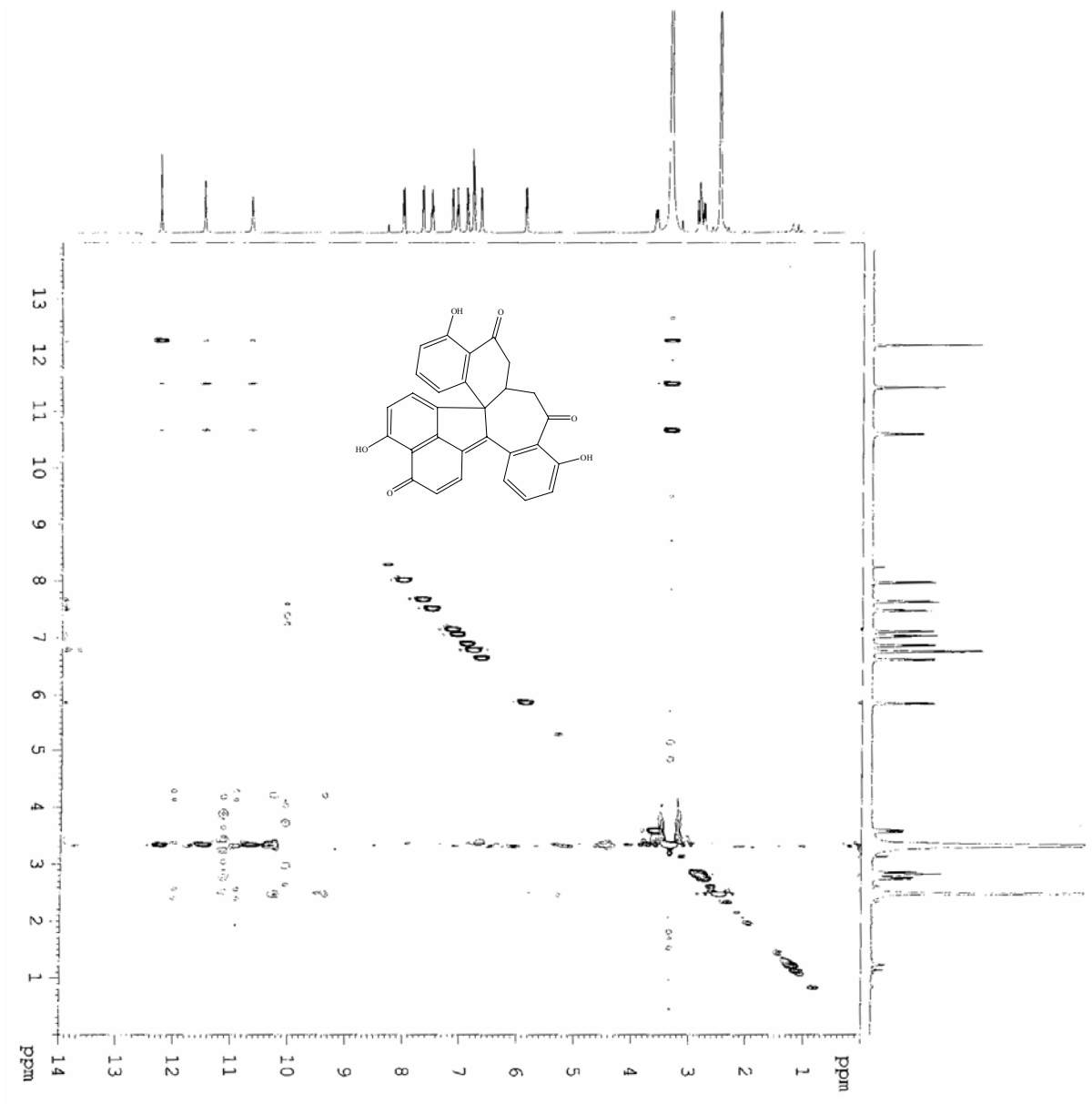

Figure S6. The NOESY spectrum of **1** in DMSO-d_6 (500MHz).

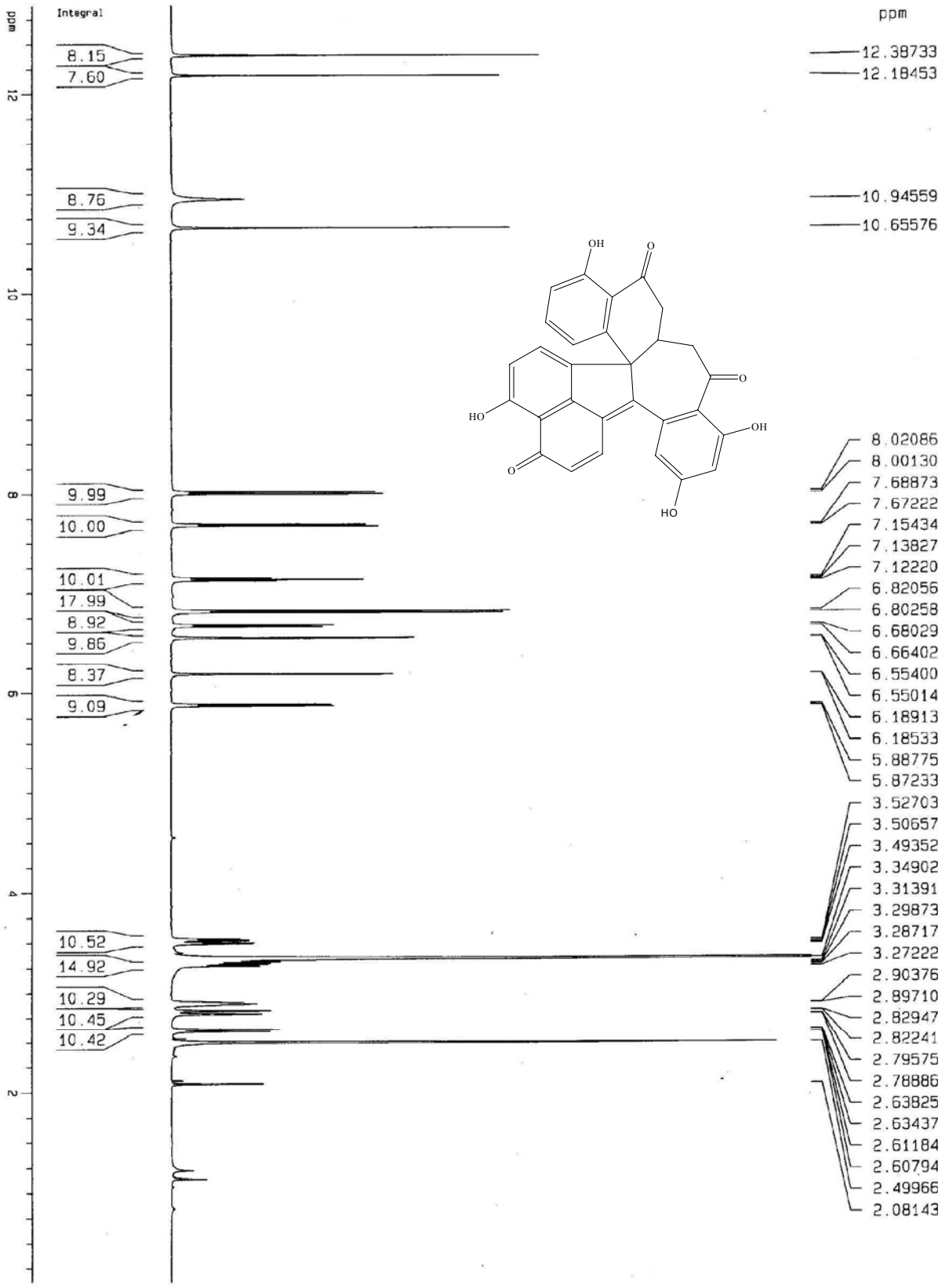

Figure S7. The ^{1}H NMR spectrum of **2** in DMSO-d_6 (500MHz).

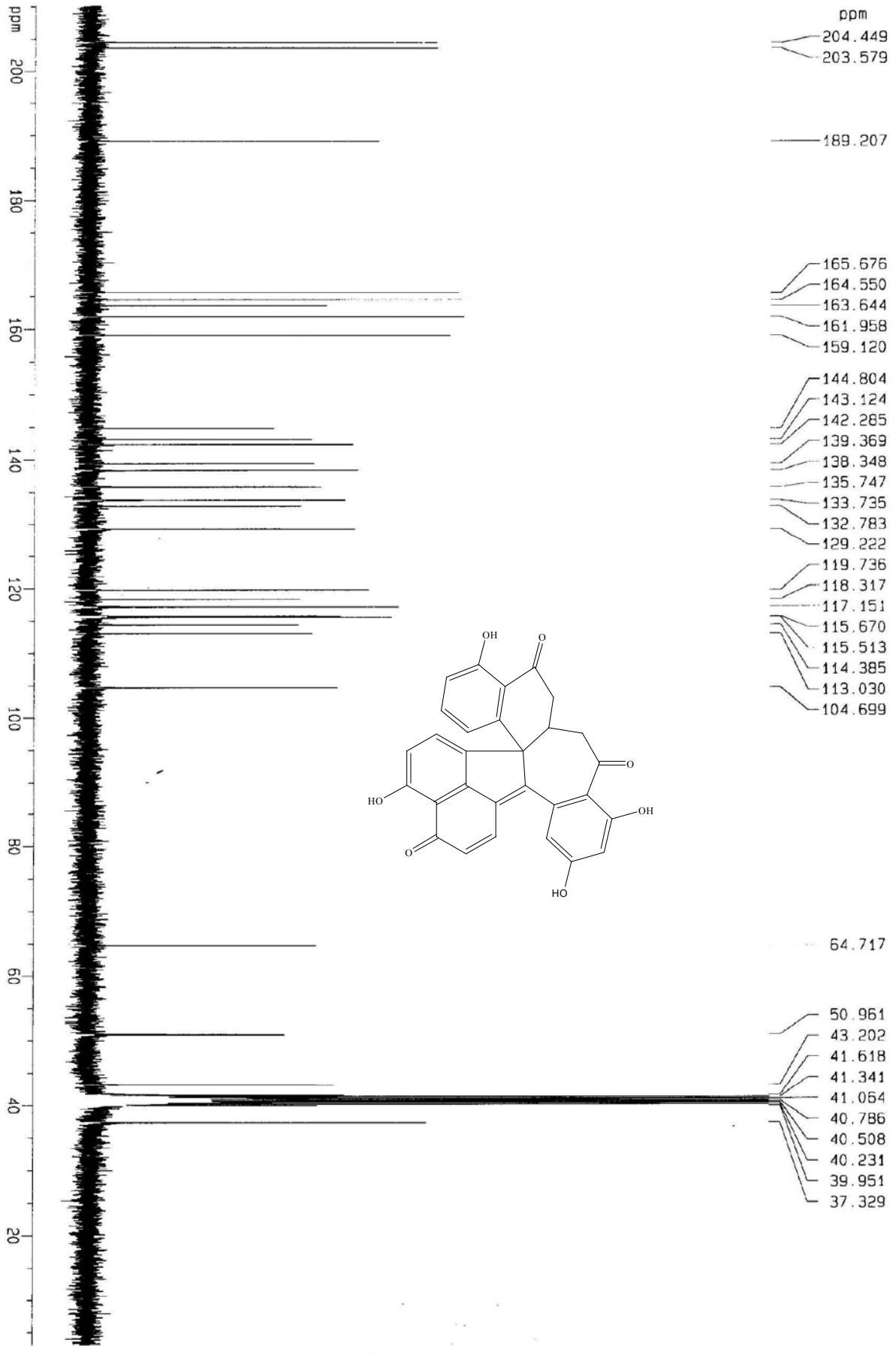

Figure S8. The ^{13}C NMR spectrum of **2** in DMSO-d_6 (75MHz).

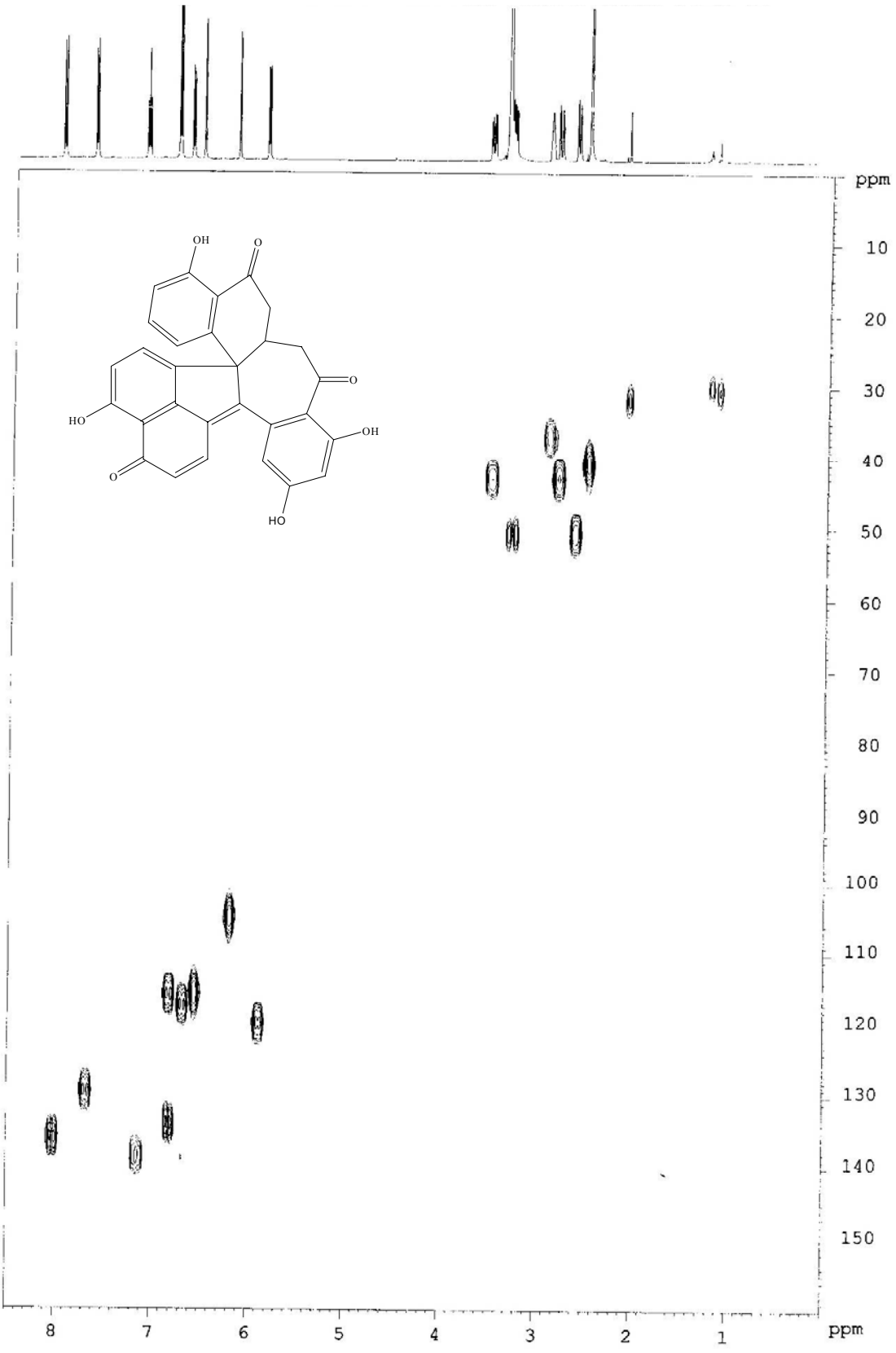

Figure S9. The HMQC spectrum of **2** in DMSO-d_6 (500MHz).

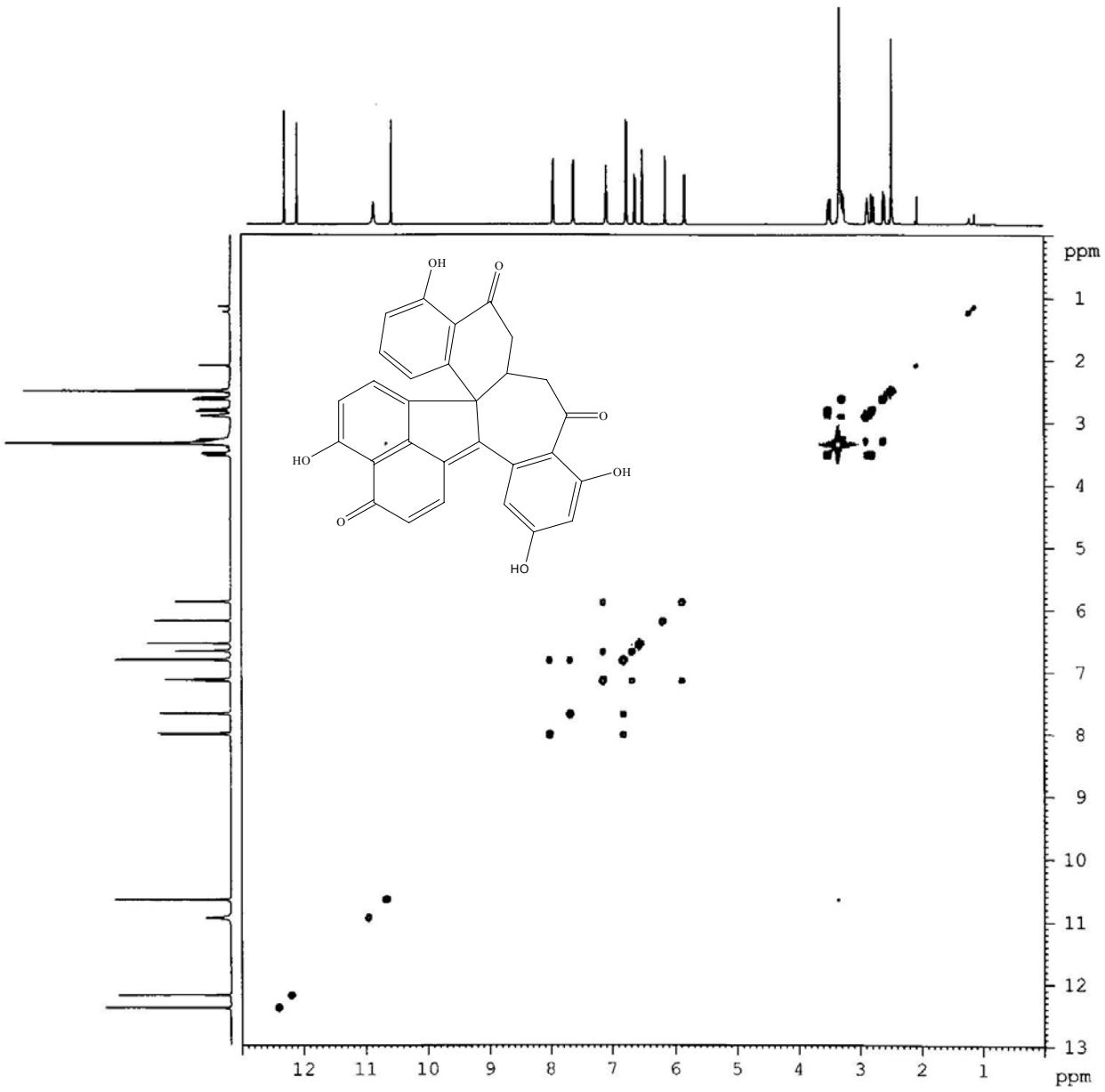

Figure S10. The ^{1}H-^{1}H COSY spectrum of **2** in DMSO-d_6 (500MHz).

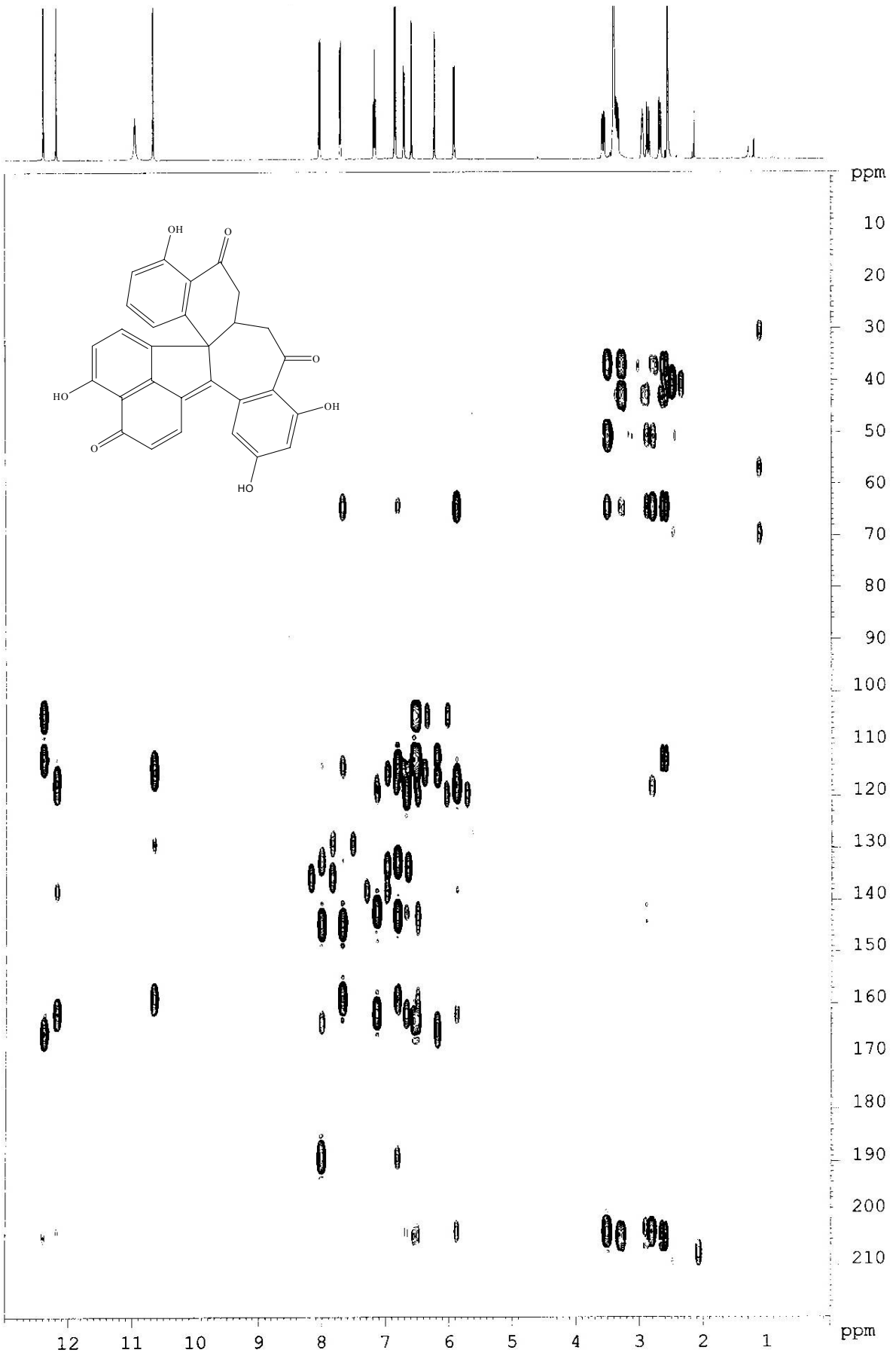

Figure S11. The HMBC spectrum of **2** in DMSO-d_6 (500MHz).

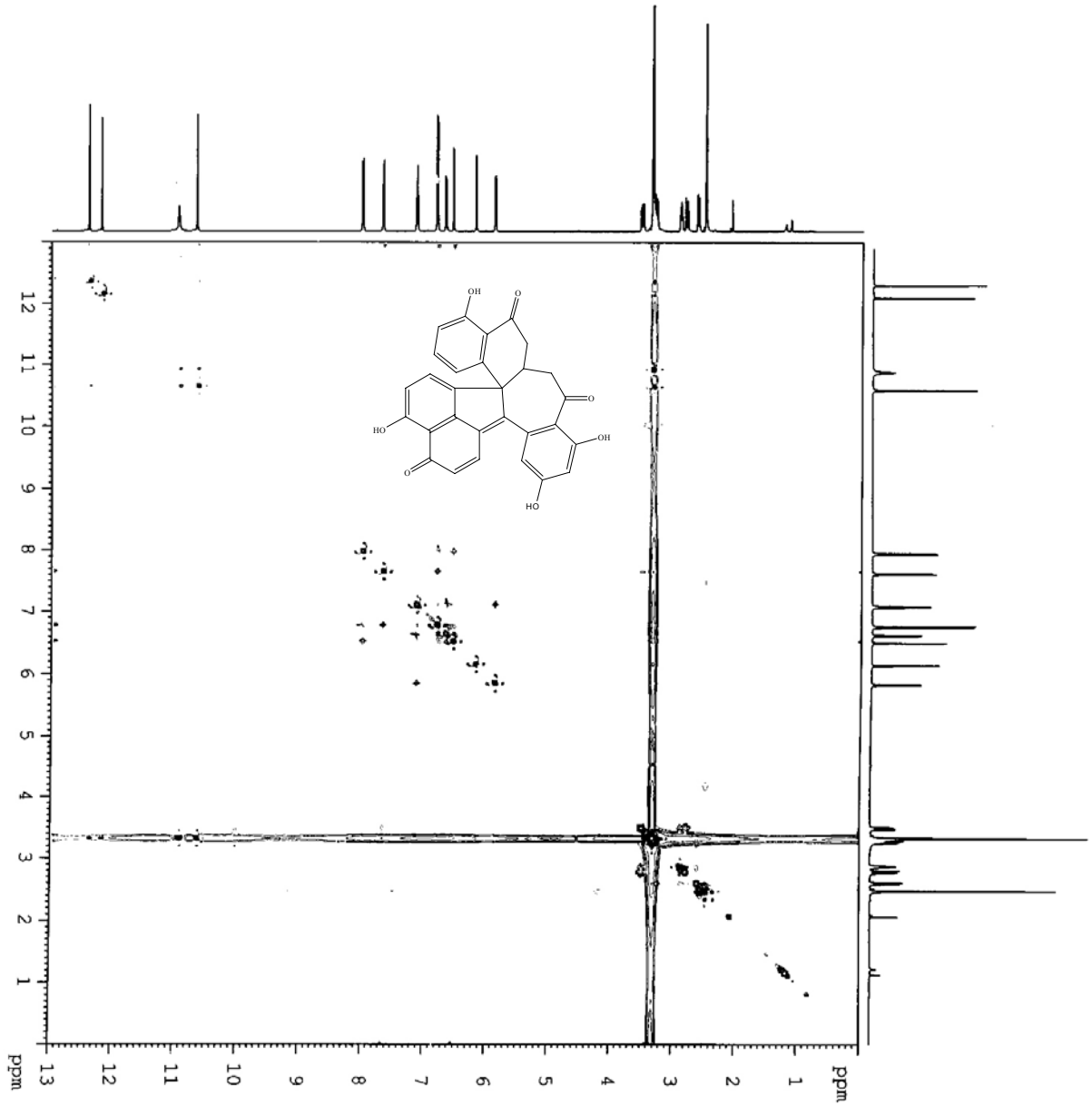

Figure S12. The NOESY spectrum of **2** in DMSO-d_6 (500MHz).

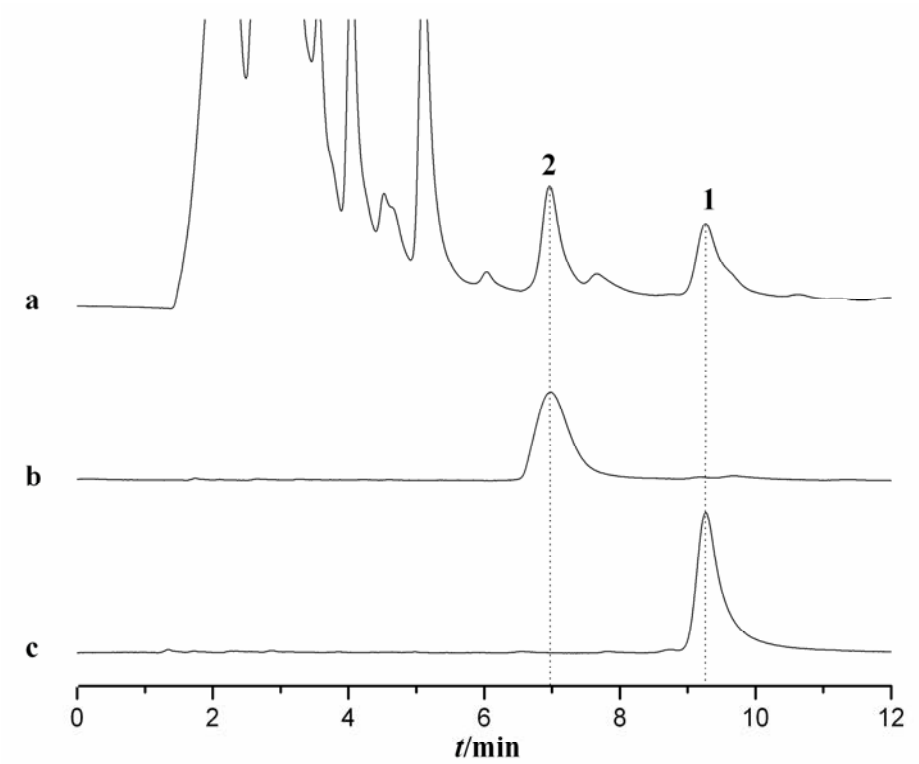

Figure S13. Normal reverse-phase HPLC analysis of the freshly prepared extract (column: Allsphere ODS-2.5 mm (250×4.6 mm), Hitachi pump L-7100, UV detector L-7400; mobile phase: MeOH/H_2O=80/20 (v/v); flow rate: 1.0 mL/min). (a) MeCN-soluble extracts, (b) dalesconol B (**2**), (c) dalesconol A (**1**).

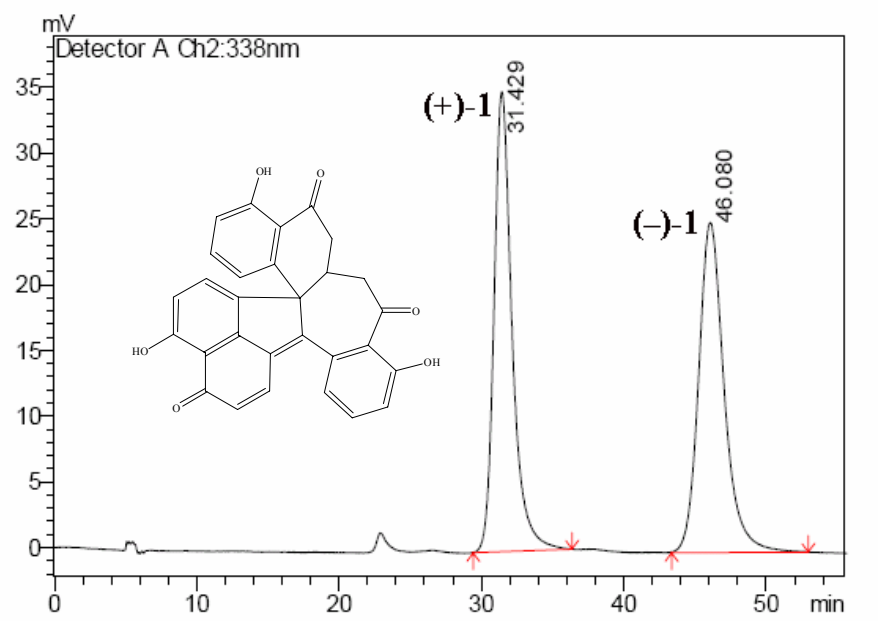

<Column Performance Report>

Peak No.	Time	Area	Area %
1	31.429	3085149	49.604
2	46.080	3134405	50.396

Figure S14. Chiral HPLC preparation chromatograms of **1** (obtained from recrystallization).

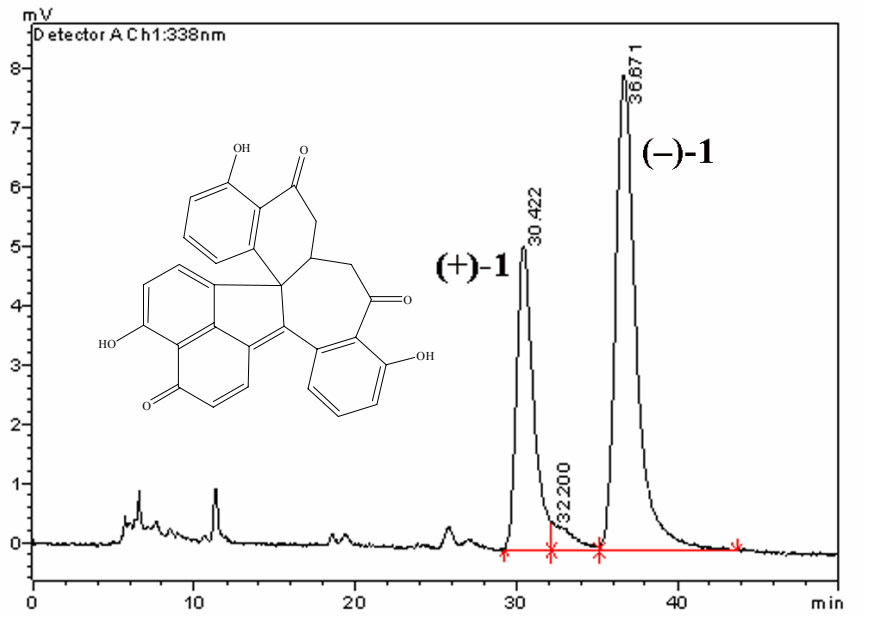

<Column Performance Report>

Peak No.	Time	Area	Area %
1	30.422	363620	33.3345
2	36.671	727203	66.6655

Figure S15. Chiral HPLC analysis chromatograms of **1** (obtained from direct HPLC collection).

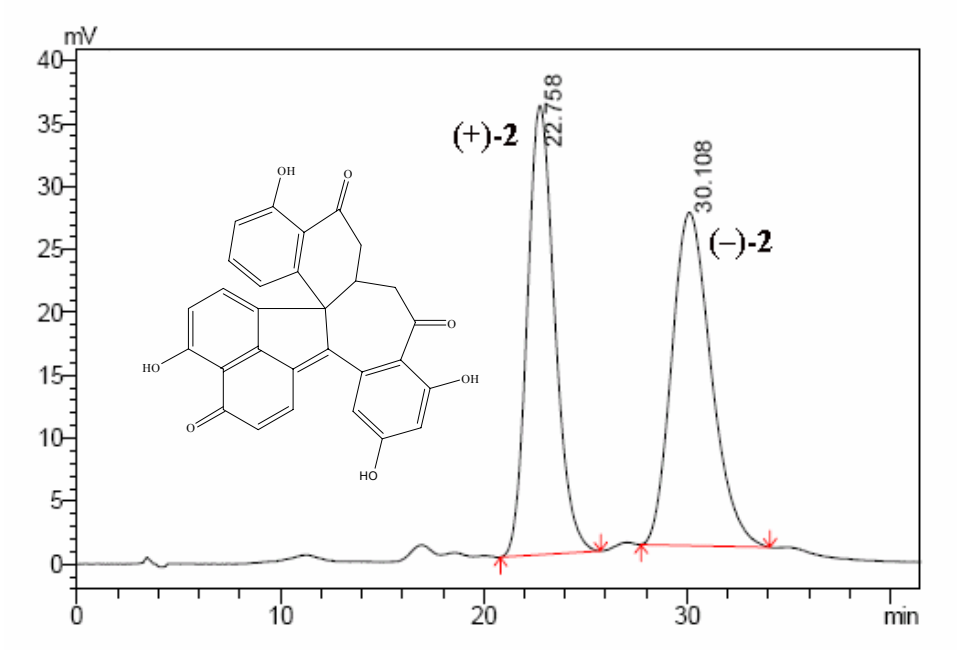

<Column Performance Report>

Peak No.	Time	Area	Area %
1	22.751	6656527	49.0645
2	30.085	6910374	50.9355

Figure S16. Chiral HPLC preparation chromatograms of **2** (obtained from recrystallization).

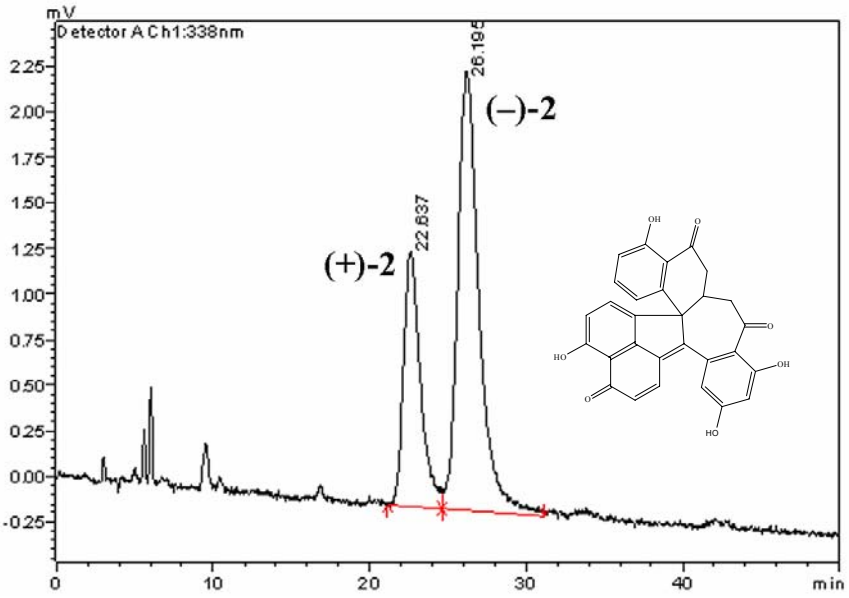

<Column Performance Report>

Peak No.	Time	Area	Area %
1	22.637	101769	32.9609
2	26.195	206988	67.0391

Figure S17. Chiral HPLC analysis chromatograms of **2** (obtained from direct HPLC collection).

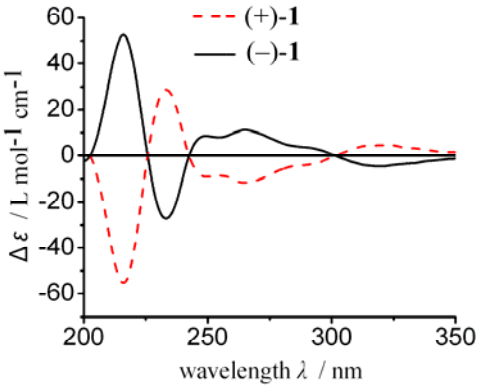

Figure S18. The CD spectra of (+)-**1** and (–)-**1** in MeCN.

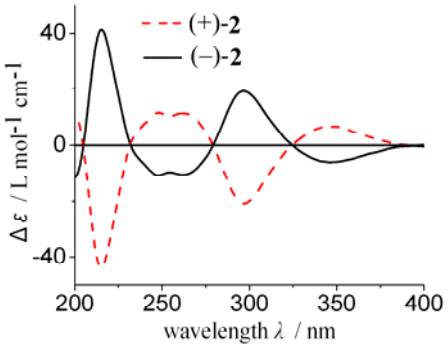

Figure S19. The CD spectra of (+)-**2** and (–)-**2** in MeCN.

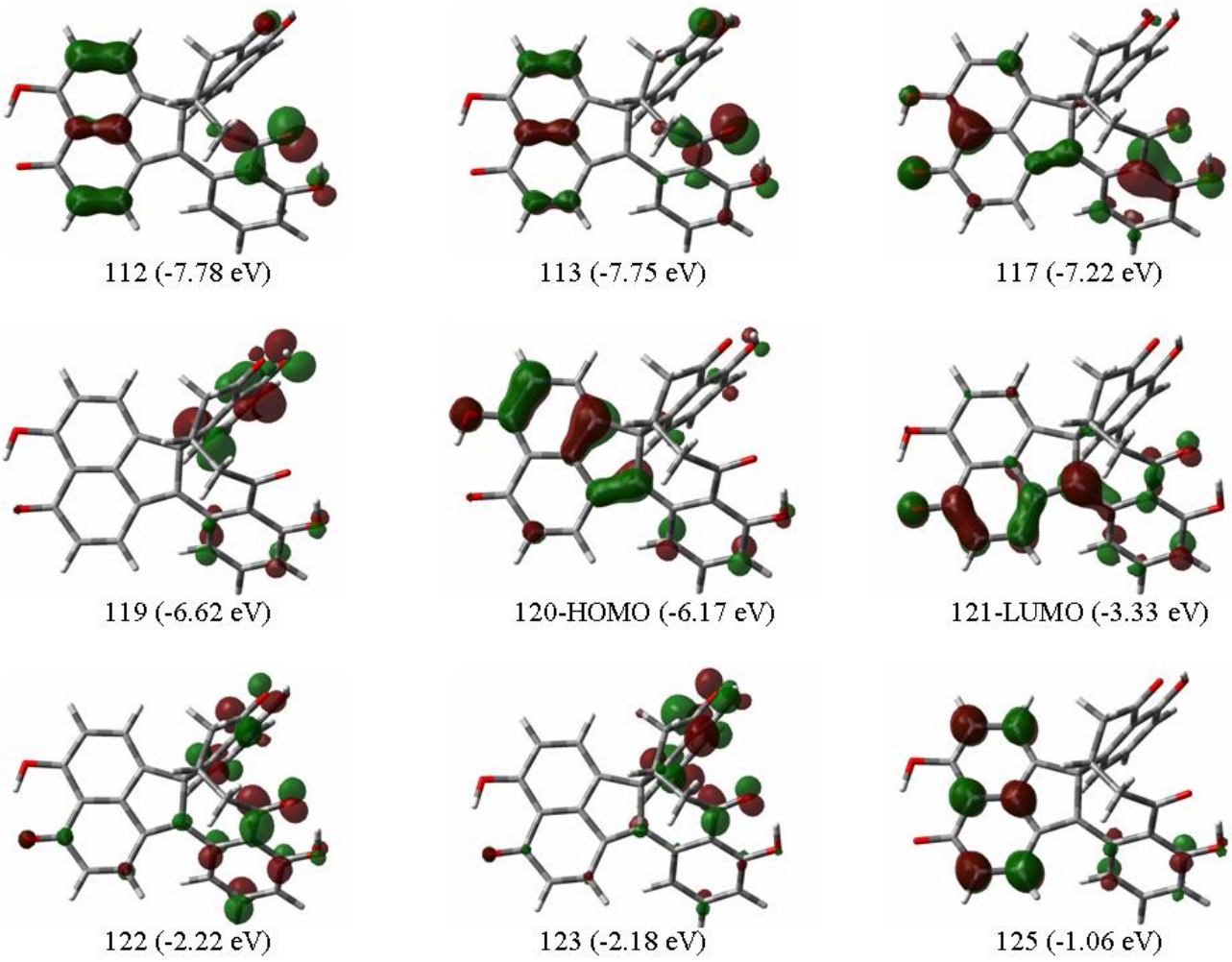

Figure S20. Plot of the most important orbitals of the optimized conformer of (–)-**1**.

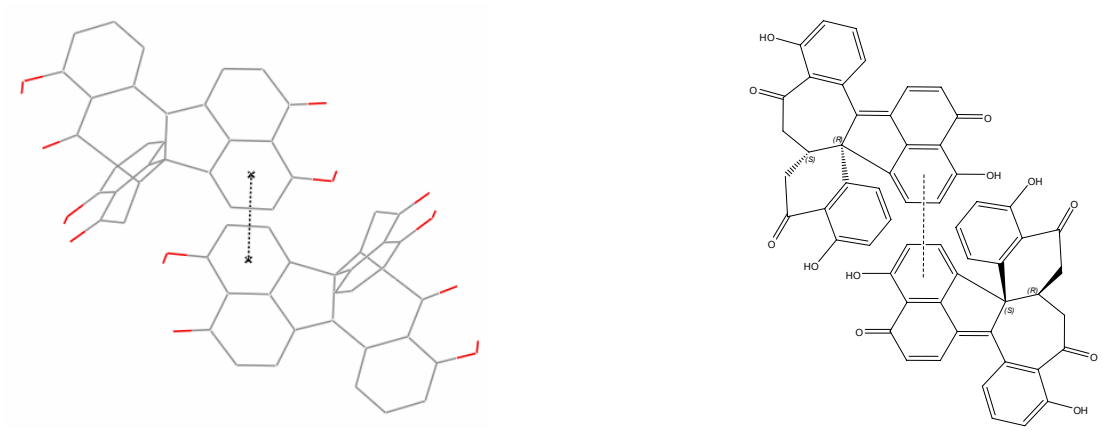

(**a**) (**b**)

Figure S21. Crystal structure (**a**) and offset π-π interaction (**b**) of dalesconol A (**1**). Hydrogen atoms omitted for clarity and the italic dashed line showing the interaction.

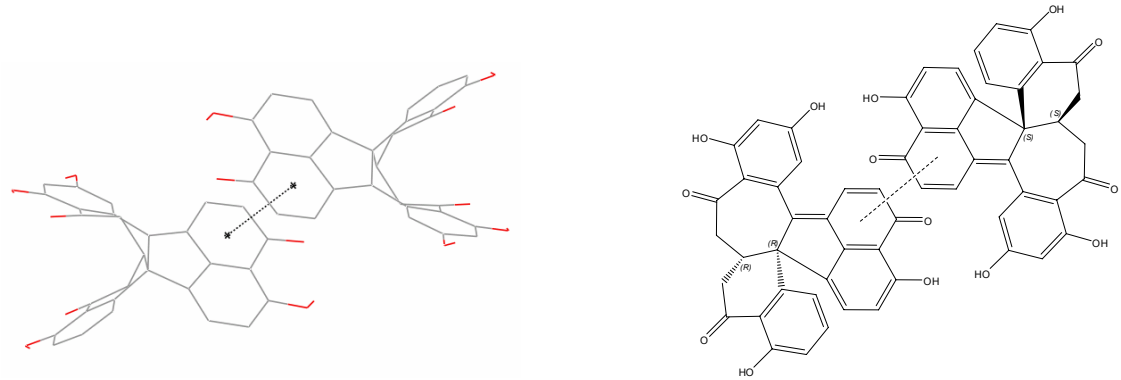

(**a**) (**b**)

Figure S22. Crystal structure (**a**) and offset π-π interaction (**b**) of dalesconol B (**2**). Hydrogen atoms omitted for clarity and the italic dashed line showing the interaction.

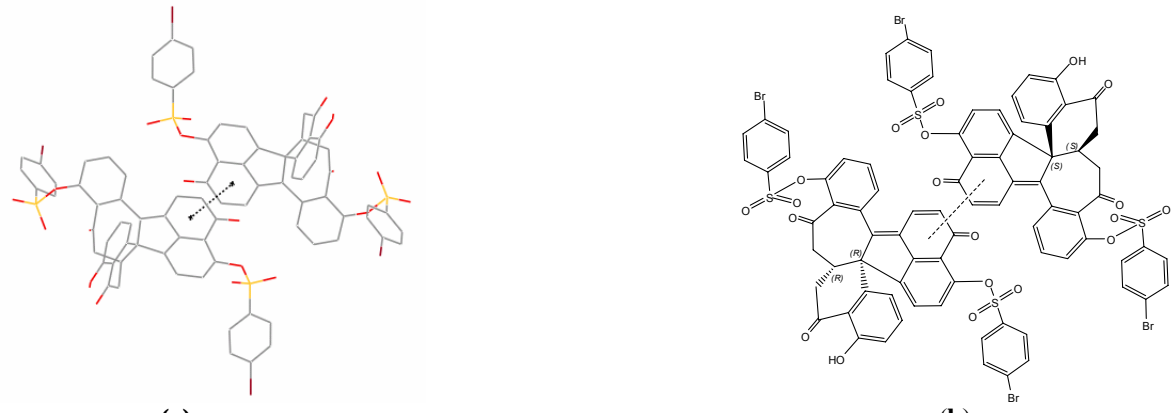

(a) (**b**)

Figure S23. Crystal structure (**a**) and offset π-π interaction (**b**) of racemic **1'**. H_2O molecules and hydrogen atoms omitted for clarity, and the italic dashed line showing the interaction.

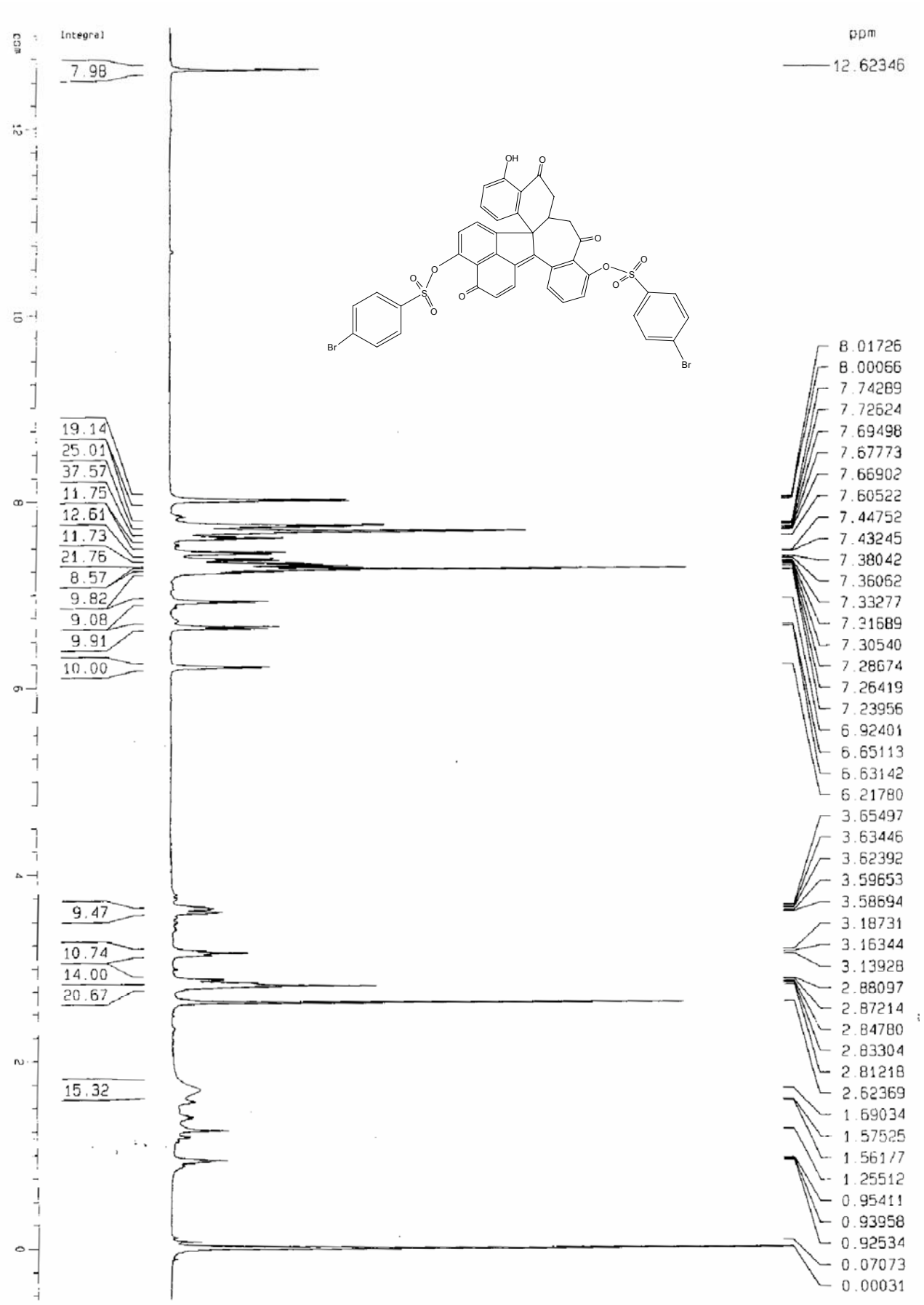

Figure S24. The ^{1}H NMR spectrum of **1'** in $CDCl_3$ (500MHz).

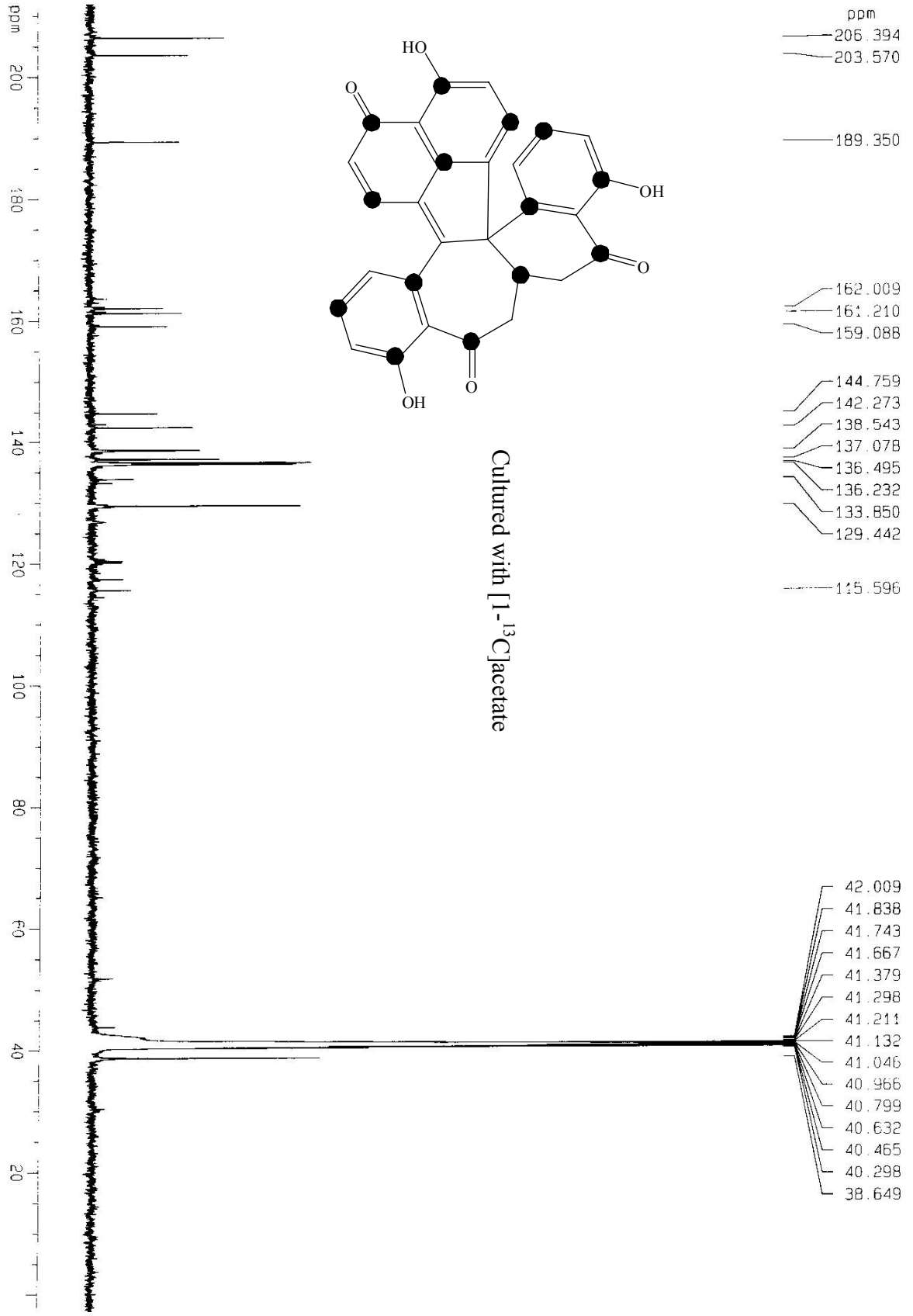

Figure S25. The ^{13}C NMR spectrum of **1a** in DMSO-d_6 (125MHz).

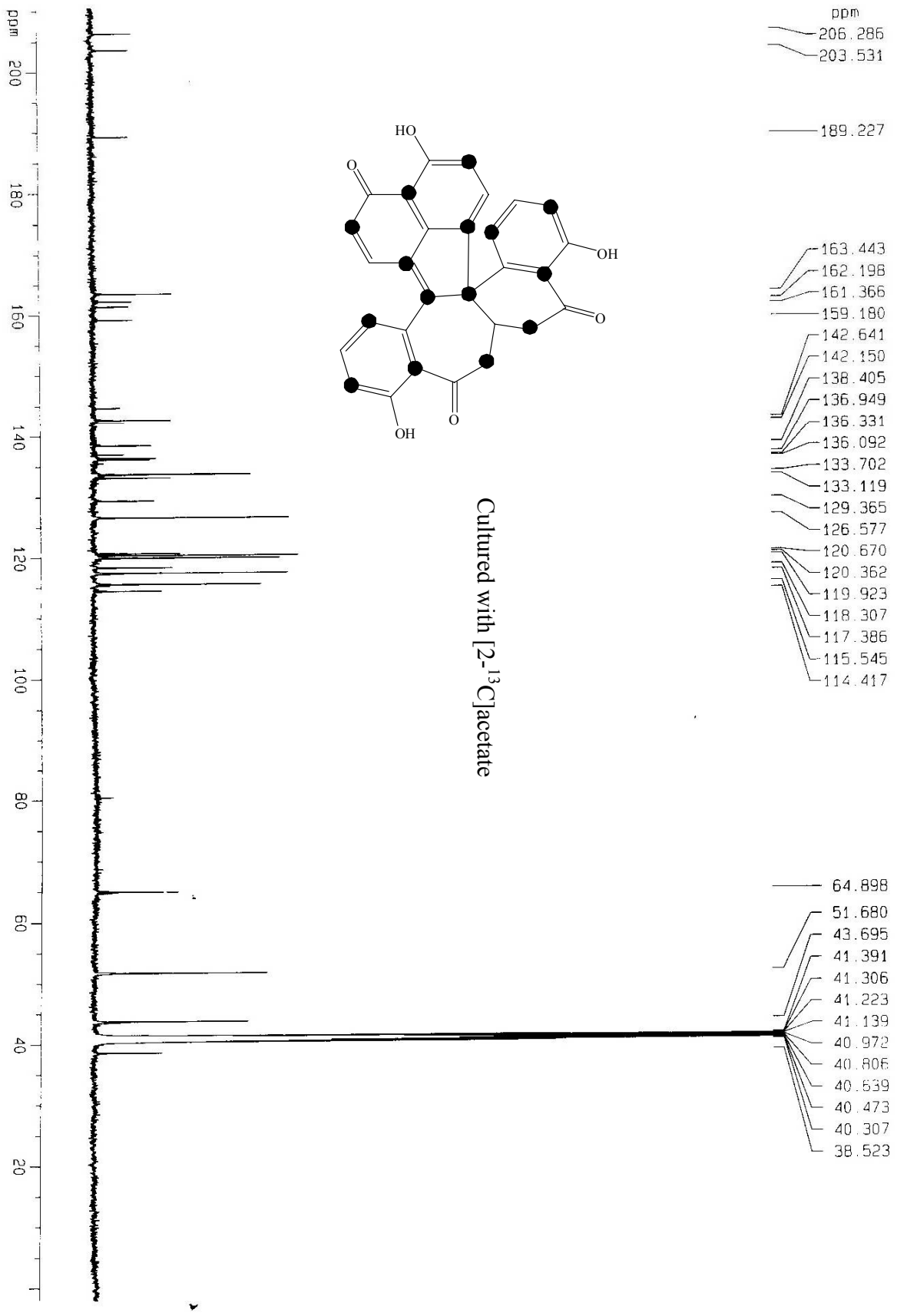

Figure S26. The ^{13}C NMR spectrum of **1b** in DMSO-d_6 (125MHz).

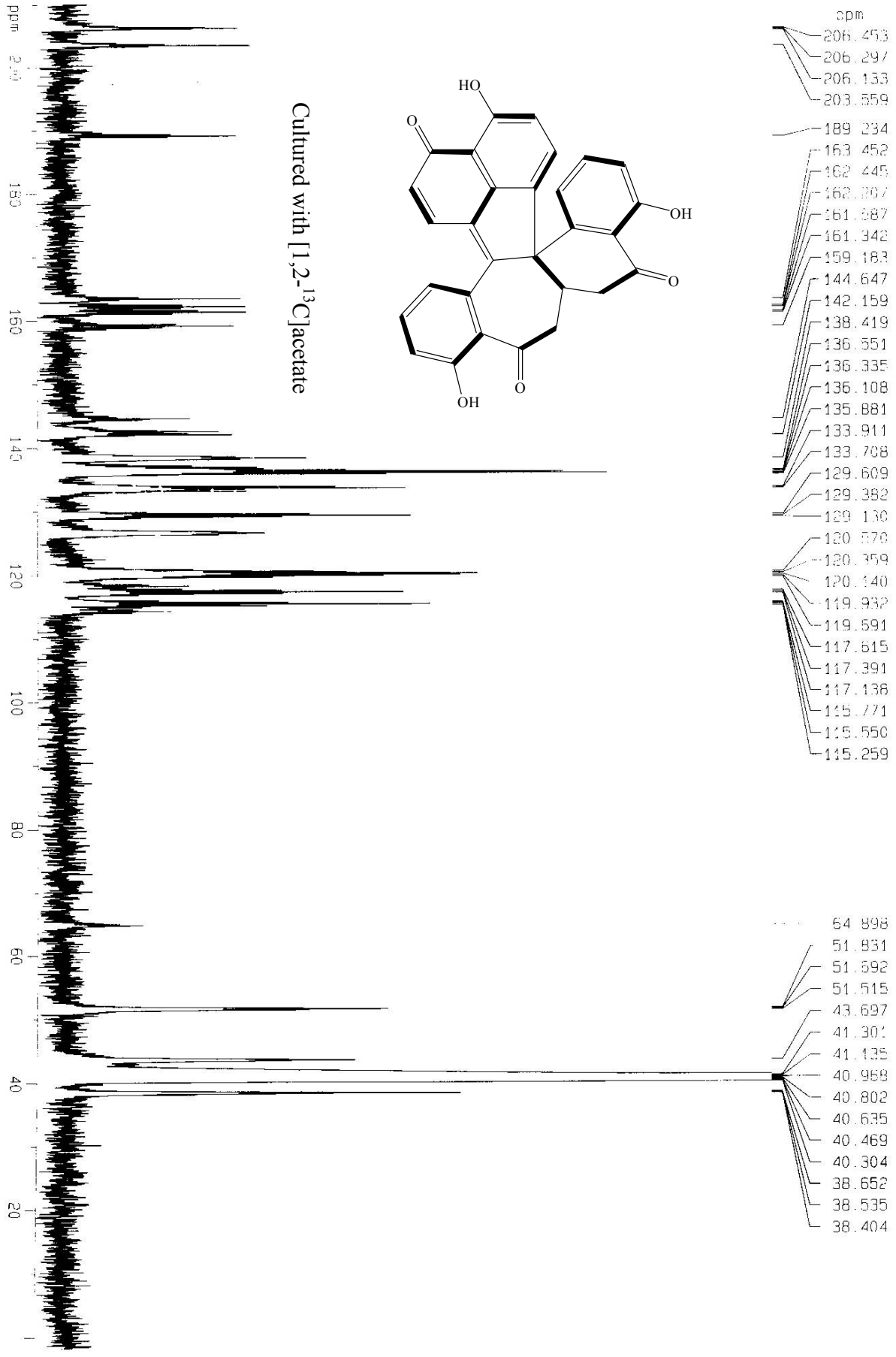

Figure S27. The ^{13}C NMR spectrum of **1c** in DMSO-d_6 (125MHz).

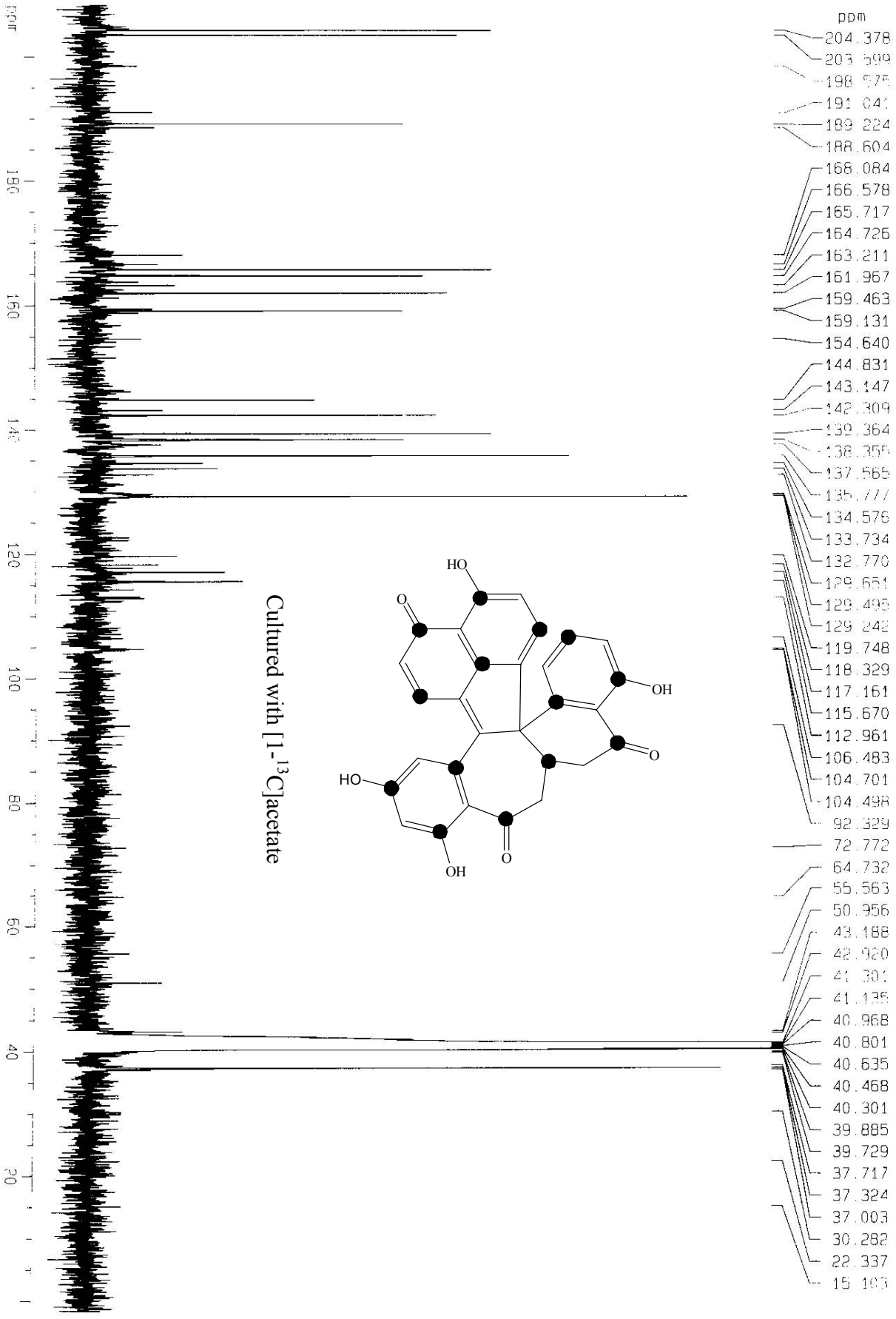

Figure S28. The ^{13}C NMR spectrum of **2a** in DMSO-d_6 (125MHz).

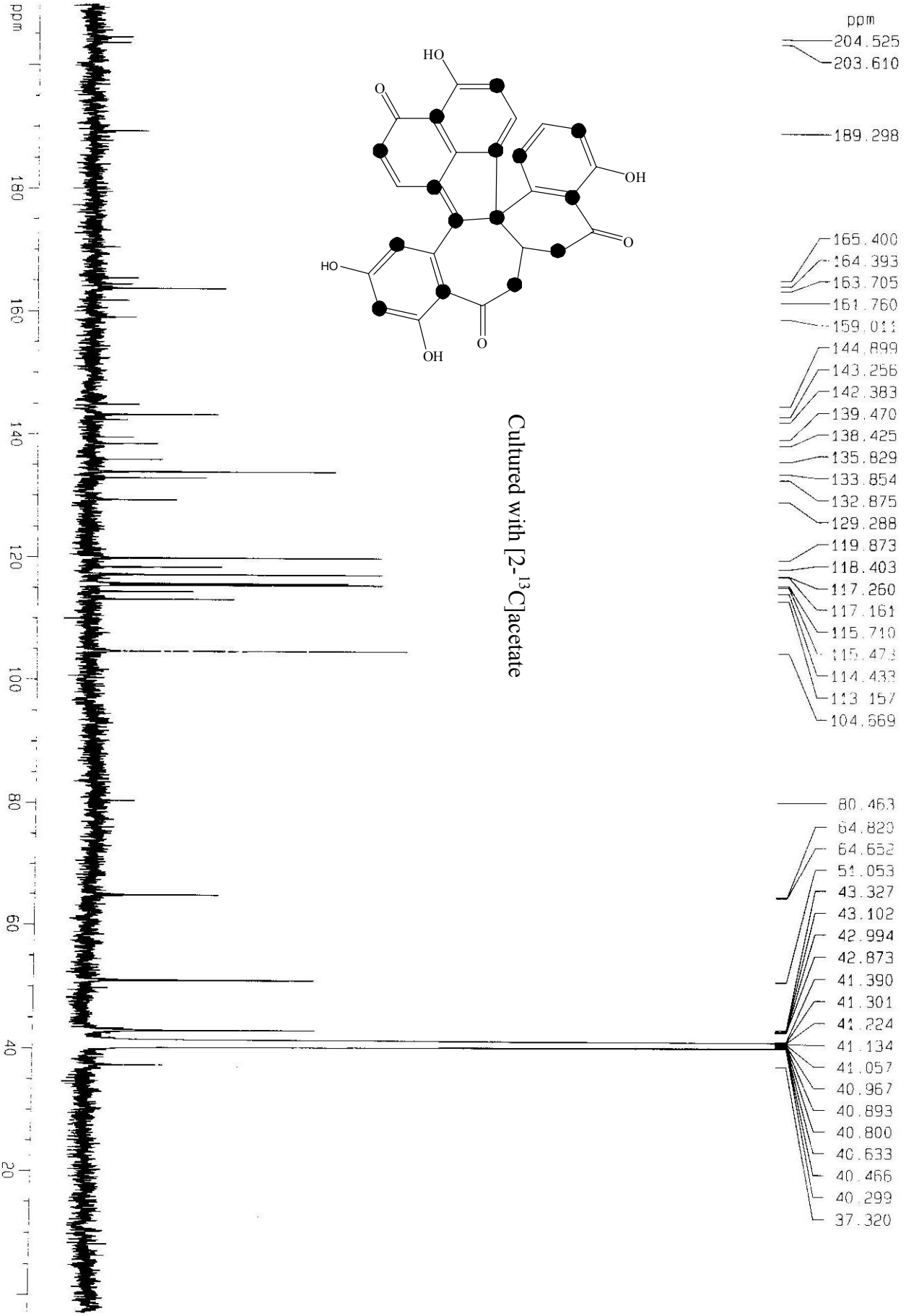

Figure S29. The ^{13}C NMR spectrum of **2b** in DMSO-d_6 (125MHz).

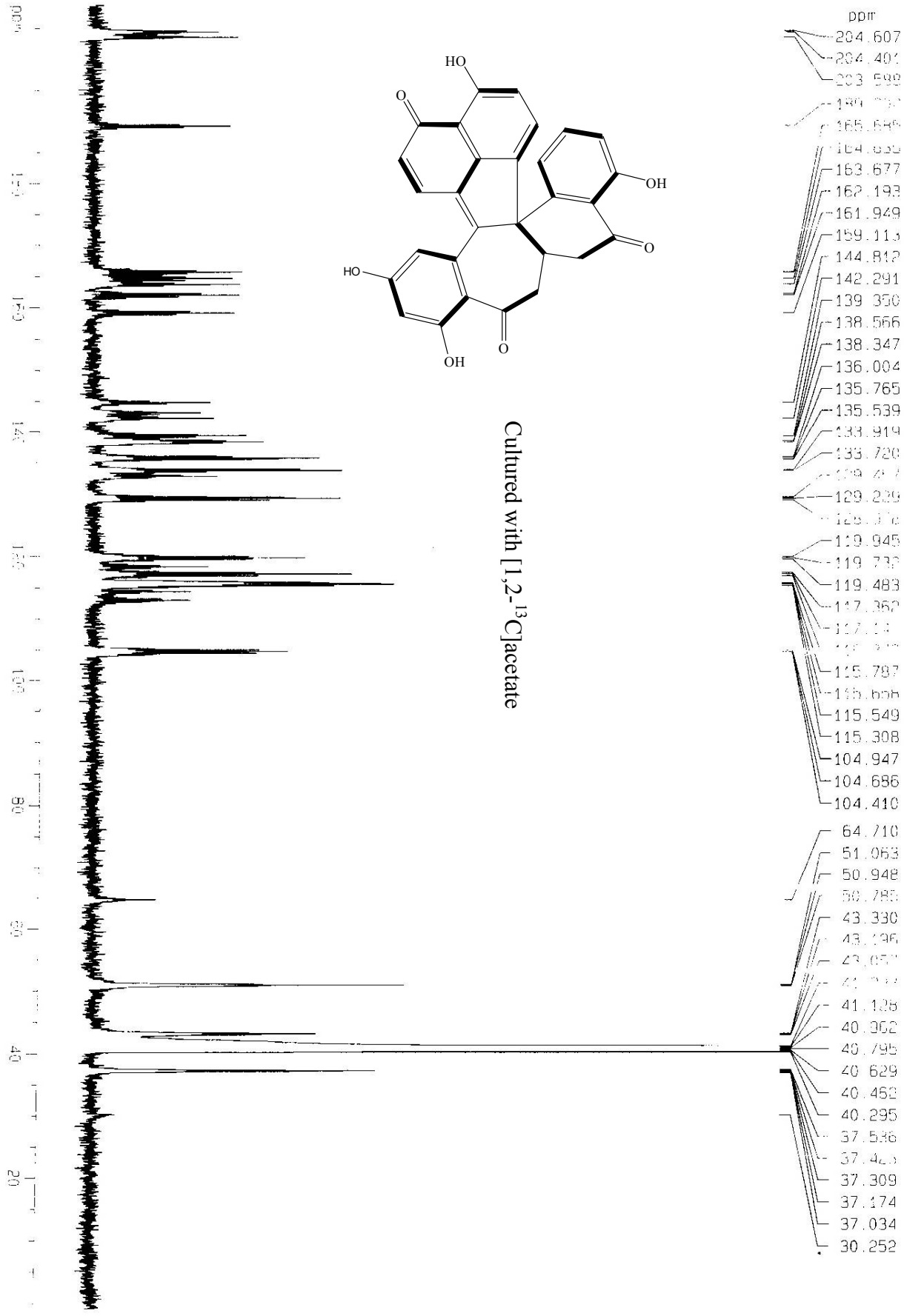

Figure S30. The ^{13}C NMR spectrum of **2c** in DMSO-d_6 (125MHz).

References for Supporting Information:

[1] a) J. M. Lindh, O. Terenius, I. Faye, *Appl. Environ. Microb.* **2005**, *71*, 7217–7223; b) S. W. Woolfolk, G. D. Inglis, *Biological. Control.* **2004**, *29*, 155–168; c) K. Matsuura, *OIKOS* **2001**, *92*, 20–26.

[2] A. Jiemchooroj, P. Norman, *Chem. Phys.* **2007**, *126*, 134102.

[3] TURBOMOLE (Version 5.8), R. Ahlrichs, M. Bär, H. P. Baron, R. Bauernschmitt, S. Böcker, P. Deglmann, M. Ehrig, K. Eichkorn, S. Elliott, F. Furche, F. Haase, M. Häser, H. Horn, C. Hättig, C. Huber, U. Huniar, M. Kattannek, A. Köhn, C. Kölmel, M. Kollwitz, K. May, C. Ochsenfeld, H. Öhm, H. Patzelt, O. Rubner, A. Schäfer, U. Schneider, M. Sierka, O. Treutler, B. Unterreiner, M. V. Arnim, F. Weigend, P. Weis, H. Weiss, University Karlsruhe, Karlsruhe, Germany, **2006**.

[4] L. Shen, Y. H. Ye, X. T. Wang, H. L. Zhu, C. Xu, Y. C. Song, H. Li, R. X. Tan, *Chem. Eur. J.* **2006**, *12*, 4393 – 4396.

[5] J. Li, J. Chen, C. S. Gui, L. Zhang, Y. Qin, Q. Xu, J. Zhang, H. Liu, X. Shen, H. L. Jiang, *Bioorgan. Med. Chem.* **2006**, *14*, 2209–2224.